



# 1 Sediment Quality Assessment in an industrialized Greek coastal 2 marine area (West Saronikos Gulf)

3 Georgia Filippi<sup>1</sup>, Manos Dassenakis<sup>1</sup>, Vasiliki Paraskevopoulou<sup>2</sup>

4 <sup>1</sup>Department of Chemistry, National and Kapodistrian University of Athens, Athens, 15784, Greece

5 <sup>2</sup>Laboratory of Environmental Chemistry, Athens, 15784, Greece

6  
7 Correspondence to: Georgia Filippi (mphilippi@chem.uoa.gr)  
8

9 **Abstract.** Eight sediment cores from the coastal marine area of West Saronikos Gulf have been analyzed for their grain size  
10 and geochemistry. The concentrations of eight metals (Al, Fe, Mn, Cu, Cr, Ni, Pb and Zn) along with total organic carbon  
11 (TOC) and carbonate content were measured. In cores taken at the deeper stations (above 100m) the analyses were  
12 performed only in the prevailing fine fraction ( $f < 63\mu\text{m}$ ) while in cores from shallow stations (below 100m) the analyses  
13 were performed separately in both fractions fine and coarse ( $63\mu\text{m} < f < 1\text{mm}$ ). The cores are fairly homogeneous, in terms  
14 of carbonates and the down-core variability of % TOC, is characterized by high surficial values that decrease with depth.  
15 Metals from both geological origin (Al, Mn, Cr, Ni) and anthropogenic origin (Cu, Pb, Zn), are higher at the silt and clay  
16 fraction of sediments than the sand fraction. The spatial distribution of Al, Fe, Mn, Cu, Pb and Zn in surface sediments  
17 presents increasing concentrations from the northeast to the southwest part of the study area, from the shallow to the deeper  
18 parts in contrast to Cr and Ni which are increased in the northern nearshore stations. Based on the vertical distributions, the  
19 metal to Al ratios of Cu, Pb and Zn show a constant decrease over depth along most cores, indicating the anthropogenic  
20 effects to surface sediments, while Fe/Al is constant. Spearman's correlation analysis performed among the fine grain metal  
21 contents, demonstrated a strong positive correlation ( $r > 0.5$ ,  $p < 0.05$ ) between Fe, Mn, Cu and Cu, Pb, Zn. Moreover,  
22 increased enrichment factors were determined at the fine fraction ( $f < 63\mu\text{m}$ ) of some sediments. The concentrations of Cr at  
23 most surface sediments are higher than the ERL value ( $81 \text{ mg Kg}^{-1}$ ) but below the ERM value ( $370 \text{ mg Kg}^{-1}$ ) and the  
24 concentrations of Ni are higher than the ERM value ( $51.6 \text{ mg Kg}^{-1}$ ). Moreover, the concentrations of Cu, Pb, Zn, at most  
25 surface sediments, are below ERL values. The mean effects range medium quotients (mERMq) of surface sediments, based  
26 on the overall metal concentrations indicated that the surface sediments of most cores, are moderately toxic. The levels of Cr,  
27 Ni, Mn and Zn at most stations are decreased in 2017, but the concentrations of Pb and Cu are increased in 2017, compared  
28 to a previous study of 2007. The concentrations of Cu, Pb and Zn in the surface sediments of West Saronikos Gulf are lower  
29 than levels reported for Inner Saronikos Gulf and Elefsis Gulf, owing to the smaller industrial zone at the western coast,  
30 compared to the numerous polluting activities at the east coast of Saronikos.

31  
32

## 33 1 Introduction

34

35 Sediment cores are one of the most easily accessed natural archives, used to evaluate and reconstruct historical pollution  
36 trends in aquatic environments. The cores provide data to characterize sediment physical properties and their geochemistry  
37 and composition. Vertical profiles of heavy metals can present sedimentation rate, changes in diagenetic processes and  
38 effects of human pressures. Metals released into aquatic systems, undergo several processes, such as adsorption, photolysis,  
39 chemical oxidation and microbial degradation. Sedimentation depends on the contaminant physicochemical properties, the  
40 sediment physical properties, the adsorption capabilities and the partitioning constant at the water-sediment interface. Trace



41 metals removed from the water column are adsorbed on particulate matter and eventually deposited on bottom sediments  
42 (Bigus et al, 2014).

43 Sediments are repositories for metals such as chromium, lead, copper, nickel, zinc and manganese that present as discrete  
44 compounds, ions held by cation-exchanging clays, bound to hydrated oxides of iron and manganese, or chelated by insoluble  
45 humic substances. Solubilization of metals from sedimentary or suspended matter depends on the presence of complexing  
46 agents. Metals that are held by suspended particles and sediments are less available than those in true solution (Manahan,  
47 2011).

48 The Saronikos Gulf is situated at the central Aegean Sea (north east Mediterranean) between 37°30'N-38°00'N and 24°01'  
49 E-23°00' E. The length of its coastline is 270 km, the surface is 2.866 km<sup>2</sup> and the mean water depth 100 m. To the north, a  
50 shallow (30 m depth) embayment is formed, known as Elefsis bay. The islands of Salamina and Aigina and the plateau  
51 between them, divide the gulf into two basins: the western basin (Western Saronikos Gulf) with maximum depths of 220 m  
52 in the north and 440 m in the south (Kontoyiannis, 2010) and the eastern basin which has a smooth bathymetry with depths  
53 of 50-70 m to the north (inner Saronikos Gulf) reaching 200 m to the southeast, from where the gulf opens to the Aegean Sea  
54 (outer Saronikos Gulf). To the west, the narrow Isthmus of Corinth connects Korinthiakos Gulf in the Ionian Sea with  
55 Saronikos Gulf in the Aegean Sea.

56 The gulf is subjected to a strong seasonal cycle of heating and cooling, with air temperatures between 0 - 40 ° C, which  
57 causes the formation of a seasonal pycnocline from May to November. In winter, the water column is homogenized down to  
58 120 m. However, in the western part, vertical mixing never reached the sea bottom (440 m) in the years after 1992 and  
59 dissolved oxygen concentration has approached nearly anoxic conditions (D.O. < 1mL/L) (Paraskevopoulou et al., 2014).

60 The gulf is subjected to intense anthropogenic pressure, as it is the marine border of the cities of Athens and Piraeus with 3-4  
61 million inhabitants. Moreover, several point and non-point pollution sources are present. One of the most important point  
62 sources is the Athens/Piraeus wastewater treatment plant (WWTP) on the small island of Psittalia, one of the largest in  
63 Europe, with a population equivalent (p.e.) coverage of 5.6 million p.e. Other point sources along the coasts include marinas,  
64 touristic facilities, fish farms and the effluents of smaller towns and settlements (Paraskevopoulou et al., 2014).

65 The coastal marine area of the north part of West Saronikos Gulf is affected by a few types of industries established there  
66 during the 1970's, that include an oil refinery unit at the center of Susaki area, a cable manufacturer, soya mills and sulfur,  
67 fertilizers manufacturing for agricultural use and the activate wastewater treatment plant of Aghioi Theodoroi. Moreover, the  
68 increased touristic activities in the nearby coastal villages, especially during the summer months (Kelepertsis et al., 2001;  
69 Paraskevopoulou, 2009) are important point sources.

70 The Susaki area, which extends parallel to the northern coast of West Saronikos for about 8 Km, is known for its volcanic  
71 activity which took place during Pliocene-Quaternary. Most of the volcanic materials were transported by fluvial processes  
72 and deposited in the alluvial plains and coastal regions. The formations observed are peridotites and serpentinites, neogene  
73 deposits and Quaternary deposits. As a result, elevated values of Cr, Ni, Co, Mn, Fe in the soils and sediments of this area  
74 can be explained by the existence of the ultrabasic rocks (Kelepertsis et al., 2001).

75 The main aim of this work is to assess the levels and the distribution of several heavy metals (Al, Fe, Mn, Pb, Zn, Ni, Cr, Cu)  
76 in the sediment cores of West Saronikos, in order to discern between geological and anthropogenic origin of heavy metals  
77 and to identify the major sources of metal pollution. The second aim is to determine the evolution of marine pollution in the  
78 area by comparing the results with those of a similar study ten years ago, conducted at the Laboratory of Environmental  
79 Chemistry of the Department of Chemistry of the National and Kapodistrian University of Athens. The last aim of this work  
80 is to assess the differences between the concentrations of heavy metals in the surface sediments of the West Saronikos Gulf  
81 and the east part of the gulf.

82  
83



84 **2 Materials and methods**

85 Eight sediment cores (12-32 cm) were obtained at corresponding stations with varying depths (50-420 m) in the area of West  
86 Saronikos Gulf using a box corer. The sampling took place in 18 October 2017 with the Greek Oceanographic vessel RV  
87 *Aegaeo*. The location of West Saronikos Gulf study area and the specific station of stations are presented in Fig. 1.

88



89  
90  
91  
92  
93

**Figure 1: Location of Saronikos Gulf and sampling stations (© Google Maps 2019). Stations MOT13A, MOT16A, UN5, MOT16, UN6, UN6A and UN4 locate at the northwest part of Saronikos Gulf and station UN11 at the southwest part.**

94 Stations MOT13A, MOT16A, UN5, MOT16, UN6 (near the Susaki area) and UN4 (Megara basin), at the northwestern part,  
95 are affected by the coastal industrial zone, urbanization and touristic activities. The offshore station UN6A, at the middle of  
96 Megara basin, is probably less affected by anthropogenic activities. Finally, station UN11 locates at the southwest part of the  
97 gulf, at Epidavros basin and is affected by trawling and aquaculture.

98 The cores were stored frozen until analysis. Subsequently, they were cut in layers of 1-2cm for the top 10cm and of 2cm  
99 below 10 cm and they were stored frozen until analysis. The separated layers were then freeze-dried. The grain size  
100 treatment included dry sieving for the separation of the silt and clay fraction (<63  $\mu\text{m}$ ) from the sand fraction (> 63 $\mu\text{m}$ )  
101 (Tsoutsia et al., 2013), using Retsch stainless steel ‘Test Sieves’. The percentage of both fractions (sand and silt-clay) was



102 calculated. The percentage of total organic carbon and carbonates and the concentrations of heavy metals were determined in  
103 both sand and fine sediment, when the fraction percentage was more than 10 % of the total sediment. Table 1 presents the  
104 coordinates, the depth and the core length of sampling stations.

105

106 **Table 1. The location and depth of sampling stations and the length of each core.**

Station	Latitude N (dec.minutes)	Longitude E (dec.minutes)	Depth (m)	Length of Cores (cm)
MOT13A	37° 54.602	23° 03.184	50	12
MOT16A	37° 53.995	23° 03.080	100	32
UN5	37° 53.459	23° 04.393	140	32
MOT16	37° 54.179	23° 05.312	85	20
UN6	37° 53.455	23° 10.857	193	26
UN6A	37° 51.610	23° 15.932	165	24
UN4	37° 57.057	23° 20.331	79	22
UN11	37° 38.800	23° 15.338	420	32

107

108 The total organic carbon (TOC) content was measured using the standard Walkley method (Walkley, 1947) as modified by  
109 Jackson (Jackson, 1958) and Loring and Rantala (Loring and Rantala, 1992), which is based on the exothermic reaction  
110 (oxidation) of the sediment with potassium dichromate ( $K_2Cr_2O_7$ ) and concentrated sulfuric acid ( $H_2SO_4$ ), followed by back-  
111 titration with ferrous ammonium sulfate ( $FeSO_4$ ) and ferroine indicator.

112 The carbonate content was determined by calculating the weight difference of the sample before and after the strong  
113 effervescence caused by adding hydrogen chloride (HCl) 6 M (exothermic reaction followed by HCl gas and  $CO_2$  emission),  
114 a method modified from Loring and Rantala (Loring and Rantala, 1992).

115 The total metal contents were extracted via complete dissolution of sediment samples with an acid mixture of  $HNO_3$ - $HClO_4$ -  
116 HF (ISO-14869-1:2000) (Peña-Icart et al., 2011). Then, the total metal concentrations were determined by Flame Atomic  
117 Absorption Spectroscopy (FAAS-Varian SpectraAA-200) (Skog et al., 1998). In order to evaluate the precision and accuracy  
118 of the method for total metal analysis certified reference materials (ISE 921, 80MS, PACS-3) from Wepal, Quasimeme and  
119 NRC-CNRC were carried through the analytical procedure along with the sediment samples. Accuracy was calculated as %  
120 recovery (percentage ratio of the measured to the certified value). The precision was evaluated by replicate analysis ( $n=3$ ) of  
121 the reference materials under reproducibility conditions (different days of digestion and measurement) and the % RSD-  
122 Relative Standard Deviation (percent ratio of the standard deviation to the average concentration of the replicates) was  
123 calculated for each metal. The quality data for the total metal method show that all recoveries are between the recommended  
124 US EPA ranges (75-125 %). Moreover, the ranges of % RSD for each metal at the collected cores are presented at Fig. A1 –  
125 A15 (Appendix A).

126 All statistical treatment of data was performed by Microsoft Excel 2010. Moreover, the graphs with the vertical distributions  
127 were plotted with Microsoft EXCEL 2010 and the horizontal distributions of metals were visualized with the software  
128 package Ocean Data View (ODV) 2017. A Spearman correlation analysis that was performed with the statistical software  
129 IBM-SPSS Statistics 2020 was used to identify the significant relationship between different heavy metals, total organic  
130 carbon and carbonates.

### 131 **3 Results**

#### 132 **3.1 Geochemical results**

133 Table 2 summarizes the main findings from the determination of geochemical parameters. The grain size in cores from  
134 stations MOT16A, UN5, UN6, UN6A, UN11, is dominated by clay and silt ( $f < 63\mu m$ ), while the percentage of sand fraction  
135 ( $63\mu m < f < 1mm$ ) is lower than 10 %, which can be attributed to the depth of these stations (above 100 m). On the other  
136 hand, the grain size in cores MOT13A, MOT16, UN4 is dominated by sand, which can be explained by the shallow depth of



137 these stations (depth below 100 m) and their proximity to the northwestern coast. However, the percentages of clay and silt  
 138 in cores MOT13A, MOT16, UN4 are not negligible (above 10 %).

139 As a result, the percentages of total organic carbon (TOC) and carbonates and the concentrations of heavy metals were  
 140 determined in the fine fraction ( $f < 63\mu\text{m}$ ) of sediments in cores MOT16A, UN5, UN6, UN6A and UN11 and both in sand  
 141 and fine fraction of sediments in cores MOT13A, MOT16 and UN4.

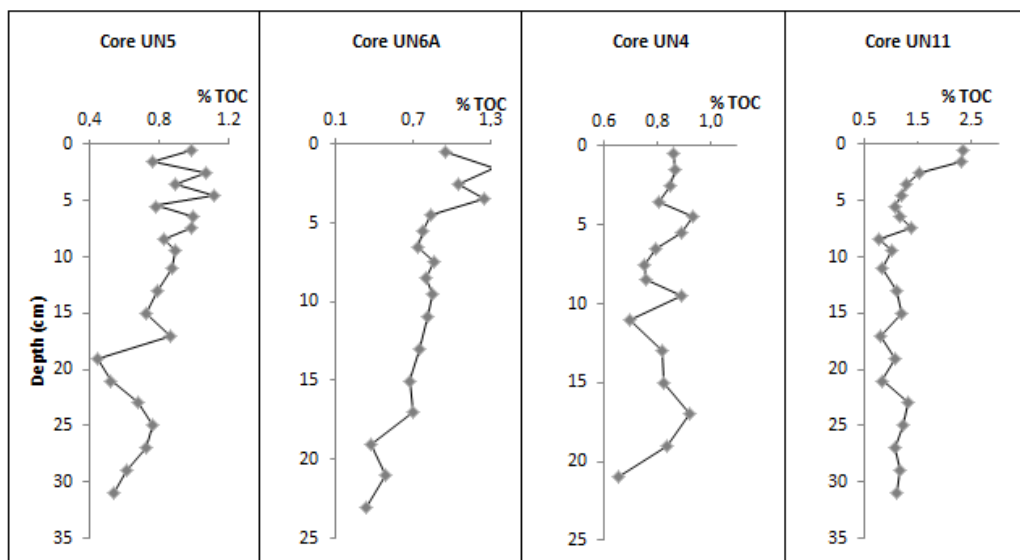
142

143 **Table 2. Summary statistics of variables measured along the collected cores.**

Station	% sand		% silt and clay		% TOC		% $\text{CO}_3^{2-}$	
	Min	Max	Min	Max	Min	Max	Min	Max
MOT13A	51	66	15	38	0.45	0.92	26	28
MOT16A	1	23	77	99	0.10	0.93	22	23
UN5	1	14	86	99	0.44	1.12	20	23
MOT16	47	65	29	45	0.33	1.28	20	22
UN6	1	32	68	99	0.57	2.44	19	23
UN6A	1	22	78	99	0.33	1.32	22	25
UN4	39	60	20	50	0.51	0.75	29	33
UN11	0	15	74	100	0.77	2.35	15	19

144

145 Apart from small variations, the cores are fairly homogeneous, in terms of carbonates. The high percentages of %  $\text{CO}_3^{2-}$  in  
 146 cores MOT13A and UN4 are associated with the coarse- grained samples and the presence of shell fragments. Moreover, the  
 147 down-core variability of % TOC at the collected cores, is characterized by high surficial values that decrease with depth.  
 148 Figure 2 presents the vertical distribution of % TOC in selected cores. The distribution at core UN4 refers to the fine  
 149 sediment fraction ( $f < 63\mu\text{m}$ ).



150

151 **Figure 2: Vertical distribution of % TOC at cores UN5, UN6A, UN4, UN11. The distribution at core UN4 refers to the fine**  
 152 **sediment fraction ( $f < 63\mu\text{m}$ ).**  
 153

154 Table 3 presents TOC, carbonate and heavy metal contents in the shallow coarse-grained cores MOT13A, MOT16, UN4. It  
 155 is apparent that the % TOC of the silt and clay sediment fraction is higher than the corresponding content of the sand fraction  
 156 as anticipated. The %  $\text{CaCO}_3$  content of the sand fraction is increased compared to the fine fraction in cores MOT13A, UN4  
 157 and approximately equal in the two sediment fractions of core MOT16.

158 The concentrations of Al, Cr, Cu, Mn, Pb, Ni and Zn are higher in the silt-clay sediments of MOT13A and UN4 than the  
 159 corresponding in sandy sediments. The same applies to Al, Mn, Cu, and Zn in MOT16. The high content of Al at the fine  
 160 fraction of sediments indicates that Al is predominantly associated with aluminosilicate minerals and occurs mostly in the



161 clay minerals. Generally, fine sediments tend to have relatively high trace element concentrations, due to the surface  
 162 adsorption and ionic attraction. Especially, the so-called anthropogenic trace metals (Cu, Pb, Zn) are normally bound within  
 163 or sorbed by the clay mineral fraction of sediments (Barjy et al., 2020; Karageorgis et al., 2005). Unlike other metals the Fe  
 164 content is more or less similar in both sediment fractions of cores MOT13A and UN4. The sediments of core MOT16 appear  
 165 to be different with higher concentrations of Fe, Cr, Ni and Pb in the coarse-grained fraction.

166

167 **Table 3. Percentage of organic and inorganic carbon and concentrations of metals in mg Kg<sup>-1</sup> in coarse-grained cores (MOT13A,  
 168 MOT16, UN4).**

169

Variable/Core	MOT13A		MOT16		UN4	
	fine fraction	coarse fraction	fine fraction	coarse fraction	fine fraction	coarse fraction
% TOC	0.64-2.80	0.26-0.45	0.37-2.70	0.15-0.46	0.65-0.94	0.43-0.58
% CaCO <sub>3</sub>	22-23	27-30	21-23	18-22	26-29	32-36
Al	10561-18387	6615-9226	21677-28939	10610-18538	23271-34246	10449-19765
Cr	390-651	333-486	322-374	306-517	113-133	71.6-115
Ni	293-411	220-302	314-573	424-697	139-187	78.0-140
Fe	19878-21153	17430-20643	24130-31694	32265-36080	14149-17126	13501-17931
Mn	429-476	326-386	471-530	435-484	317-366	174-238
Cu	17.1-18.8	8.9-11.8	16.7-22.6	6.7-14.8	15.1-23.6	9.7-13.4
Pb	18.0-30.7	14.8-21.0	9.1-28.0	8.3-31.9	11.2-31.2	9.3-27.3
Zn	39.3-51.8	31.0-45.6	39.8-53.7	31.5-50.9	38.9-59.2	30.3-50.3

170

171 The vertical distributions of the study metals in mg kg<sup>-1</sup> along the collected cores present at Fig. A1–A15 (Appendix A). In  
 172 cases of coarse cores MOT13A, MOT16, UN4, the concentrations of the total sediment (both fractions) are depicted.

173 Table 4 summarizes the concentrations of eight heavy metals in the surface and deeper sediment layer of the collected cores.

174 The concentrations are measured at the fine sediment fraction ( $f < 63\mu\text{m}$ ) of cores MOT13A, MOT16, UN4. The sediments  
 175 at the deeper parts of West Saronikos (cores UN6, UN6A and UN11) present elevated concentrations of Al, Fe, Pb and Zn  
 176 especially. The sediments of UN11 are also particularly enriched in Mn, which is attributed to the prevalence of the silt-clay  
 177 sediment fraction and the suboxic waters at depths higher above 200 m (Kontoyiannis, 2010). The elevated values of Cr and  
 178 Ni in cores MOT13A, MOT16 and MOT16A can be explained by the existence of the ultrabasic rocks of the Susaki area, in  
 179 which, these metals are predominant (Kelepertsis et al., 2001).

180

181 **Table 4. Concentrations in mg Kg<sup>-1</sup> of the study metals in the surface and the deeper sediment layer of cores. The concentrations at  
 182 coarse cores MOT13A, MOT16, UN4 are measured at the fine sediment fraction ( $f < 63\mu\text{m}$ ).**

183

Core	Layer (cm)	Al	Cr	Ni	Fe	Mn	Cu	Pb	Zn
MOT13A	0-1	10561	651	411	20988	476	18.2	26.1	49.6
	10-12	14673	407	383	21153	444	18.1	22.5	44.6
MOT16A	0-1	27009	280	375	23315	578	22.6	20.4	48.3
	30-32	30070	256	382	26179	562	22.1	28.1	44.1
UN5	0-1	32705	199	305	25534	635	27.4	42.7	74.5
	30-32	37885	223	320	29170	520	26.0	24.7	57.5
MOT16	0-1	21677	369	377	25816	530	22.6	28.0	53.7
	18-20	23807	348	401	29752	482	16.9	9.1	40.4
UN6	0-1	43264	142	253	27301	954	36.7	52.9	92.1
	24-26	44547	153	274	29345	707	28.5	32.5	62.4
UN6A	0-1	39314	146	187	21838	570	26.3	38.4	73.8
	22-24	41303	161	209	23827	513	25.4	38.7	58.7
UN4	0-1	34246	132	162	15762	358	23.6	26.1	52.1
	20-22	31706	113	160	17112	365	15.1	12.0	40.3
UN11	0-1	54626	142	230	32177	3925	49.7	63.9	110
	30-32	48186	163	217	31573	1459	37.3	35.1	71.4

184

185 The distribution of elements comprising the terrigenous phase of the sediments is best represented by Al, which is held  
 186 almost exclusively in terrigenous aluminosilicates (Karageorgis et al., 2005). Table A1 (appendix A) presents the ratios of  
 187 eight heavy metals to Al in the surface and deeper sediment layer of the collected cores. The ratios in coarse cores MOT13A,  
 188 MOT16, UN4 are calculated for the fine sediment fraction. The vertical profiles of ratios along the collected cores, are given

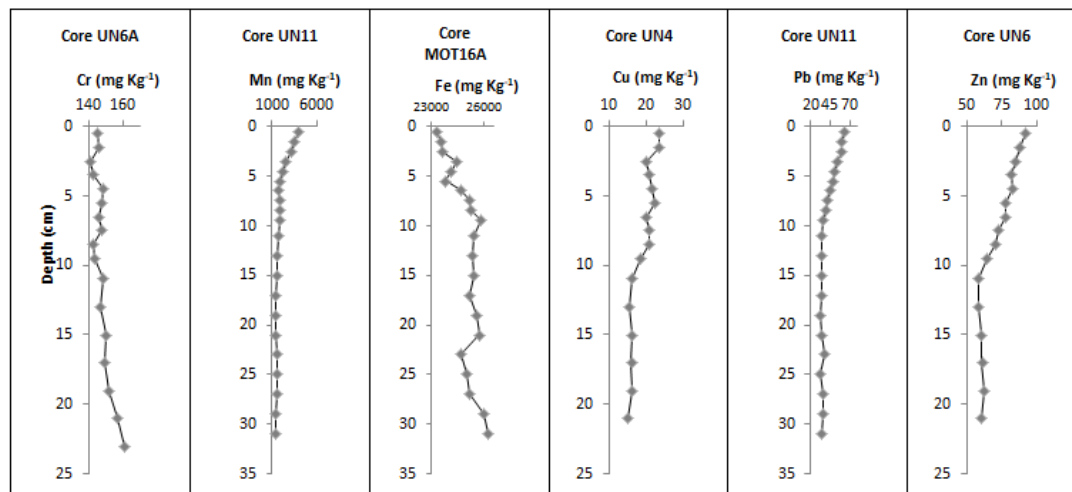




189 in Fig. A1–A15 (Appendix A), where the ratios in coarse cores MOT13A, MOT16, UN4 refer to the fine sediment fraction  
190 ( $f < 63 \mu$ ).

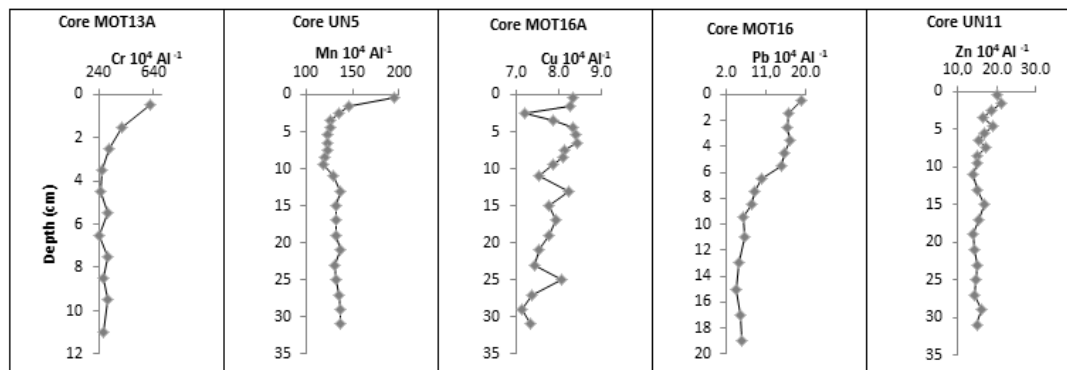
191 The vertical distributions of Al (Fig. A1 (appendix A)) for the total sediment (both fractions) present minimal variation. The  
192 down-core variability of Al is lower than 10 %, in the fine sediments (cores MOT16A, UN5, UN6, UN6A and UN11) and  
193 between 10-15 % in the coarser sediments (cores MOT13A, MOT16 and UN4). In the surface layer (0-1cm) of cores  
194 MOT13A and UN5 there is a sharp decrease of Al content, while at the top 12cm of core UN11 aluminum is increased  
195 compared to the deeper layers. Similarly, the so-called lithogenic metals (Cr, Ni, Fe, Mn) present uniform vertical profiles  
196 with minimal variability (mostly below 10 %). The trend for increase of Cr, Ni, Fe and Mn in the surface sediments of  
197 MOT13A remains pronounced after normalization to Al in silt and clay fraction at the top 0-1cm. The normalized vertical  
198 profile of Cr in UN11 indicates a decrease of Cr through time in the upper sediment layers. The same trend is seen in the  
199 normalized profiles of Ni and Mn in fine sediment fraction of core UN4. The down-core variability of Mn in all stations,  
200 except UN4, is typical of shelf sediments, with high surficial Mn concentrations that diminish with depth to background  
201 values, as reducing conditions develop. These variations are largely independent of lithological or carbonate content  
202 fluctuations, being dependent solely upon the respiration of organic carbon (Karageorgis et al., 2005).

203 The concentrations of Cu, Pb and Zn as well as the normalized profiles (Fig. A10–A15) show a constant decrease over depth  
204 to background levels, which can be attributed to increased inputs by anthropogenic activities in recent time (Karageorgis et  
205 al., 2005). Figure 3 presents selected vertical profiles of Mn and Pb along core UN11 and those of Cr, Fe, Cu, Zn at the cores  
206 UN6A, MOT16A, UN4, UN6, respectively. The concentrations were calculated at the fine fraction ( $f < 63 \mu$ ) of the  
207 sediments.



208  
209 **Figure 3: Vertical profiles of Cr, Fe, Cu, Zn at the fine fraction ( $f < 63 \mu$ ) of cores UN6A, MOT16A, UN4, UN6 respectively and**  
210 **the vertical distributions of Mn and Pb along core UN11.**  
211

212 Figure 4 presents selected vertical distributions of ratios to Al at cores MOT13A, UN5, MOT16A, MOT16 and UN11 of  
213 West Saronikos Gulf. The ratios were calculated at the fine fraction ( $f < 63 \mu$ ) of the sediments. Based on the vertical  
214 distributions, Fe to Al ratios are constant with depth of the collected cores (Nolting et al., 1999). Ration of Cu, Pb and Zn to  
215 Al show a constant decrease over depth along the collected cores, because the surface sediments are affected much higher by  
216 anthropogenic activities than the deeper sediments (Karageorgis et al., 2005).



217

218

219

**Figure 4: Vertical distributions of ratios to Al at cores MOT13A, UN5, MOT16A, MOT16 and UN11 of the northwest Saronikos Gulf. The ratios were calculated at the fine fraction ( $f < 63\mu\text{m}$ ) of the sediments of cores MOT13A and MOT16.**

220

### 3.2 Horizontal distributions

221

Figure 5 presents the horizontal distributions of heavy metals in the surface sediments (0-1 cm) of the study area. In cases of coarse surface sediments of MOT13A, MOT16, UN4, the concentrations of total sediment fraction ( $f < 1\text{mm}$ ) were used.

222

The concentrations of Al, Fe, Mn, Cu, Pb and Zn are increased from the northeast to the southwest area of West Saronikos

223

Gulf. The high content of Mn at the surface sediment of core UN11 can be explained by the prevalence of silt and clay

224

sediment fraction and the suboxic waters at the depth of 420 m (Ozturk, 1995). The waters of West Saronikos Gulf at depths

225

higher than 200 m, are suboxic (Kontoyiannis, 2010) and as a result, the slow diffusion of dissolved oxygen from the more

226

oxidizing overlying waters and the upward diffusion of dissolved Mn (II) from the pore water of anoxic surface sediments to

227

the sediment/water interface (Ozturk, 1995), cause the oxidation of dissolved Mn (II) and its precipitation as Mn (IV) oxides

228

(Pohl and Hennings, 1999).

229

230

On the other hand, the concentrations of Fe, Cr and Ni at the north part are higher than those at the south area, which can be

231

explained by the existence of the ultrabasic rocks in the soils of the region and the natural weathering and transport to the

232

coastal marine environment (Kelepertsis et al., 2001).

233

234

235

236

237

238

239

240

241

242

243

244

245

246

247

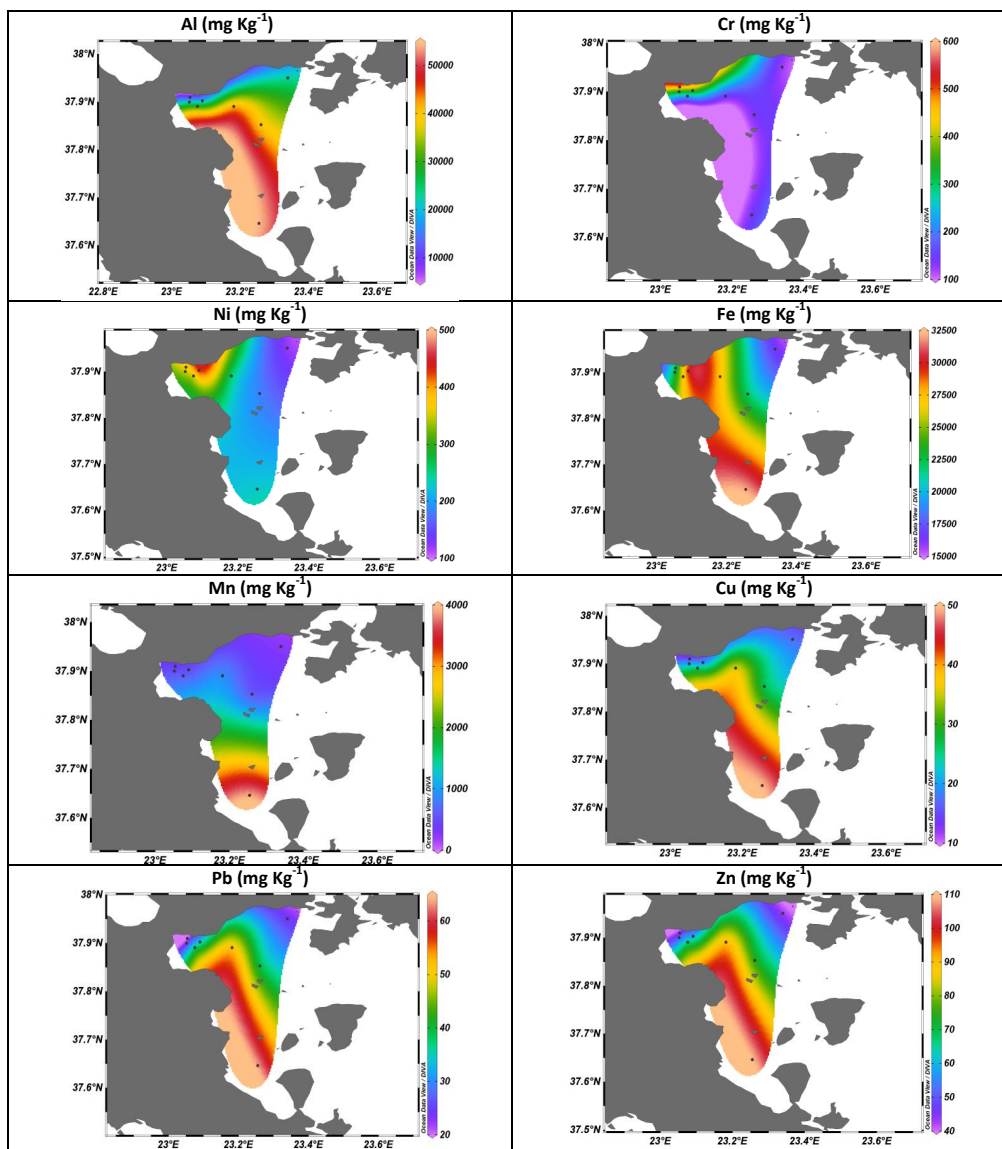
248

249





250



251

252 **Figure 5: The horizontal distributions of heavy metals in the surface sediments of West Saronikos Gulf. In cases of coarse surface**  
253 **sediments of stations MOT13A, MOT16, UN4, the concentrations of the total sediment fraction ( $f < 1\text{mm}$ ) were used.**

## 254 4 Discussion

### 255 4.1 Element interrelations

256 Spearman's correlation analysis was carried out to determine the relationships between heavy metals and percentages of  
257 total organic carbon (TOC) and carbonates in sediments of the collected cores. The concentrations of metals and the  
258 percentages of organic and inorganic carbon refer to the fine fraction of core sediments MOT13A, MOT16, UN4.  
259 Spearman's correlation coefficients are presented in Table A2 (appendix A) and Fig. A16 (appendix A).



260 Al is highly correlated ( $r > 0.5$ ,  $p < 0.05$ ) with Fe, Mn, Cu, Pb and Zn, which probably indicates an association between these  
 261 metals in the form of metal-clay complexes of continental origin (Barjy et al., 2020). On the other hand, there is a negative  
 262 correlation of Al with Cr and Ni.  
 263 Cr is highly correlated with Ni, but both of them show negative correlation with Cu, Pb and Zn, which can be attributed to  
 264 their different origin (Barjy et al., 2020) and poor correlation with Mn. Cr shows bad correlation with Fe, too. The strong  
 265 correlation between Cr and Ni can be observed at sediments of the northwest part, too.  
 266 Fe, Mn, Cu, Pb and Zn show positive correlation with each other. Cu, Pb and Zn are high correlated with each other ( $r > 0.5$ ,  
 267  $p < 0.05$ ), which can be observed at sediments of the northwest part, too, suggesting that they have a common origin and  
 268 identical behaviour during transport in the marine environment (Barjy et al., 2020). Zn is highly correlated with Cu and Pb  
 269 also at sediments of core UN11 at the south area.  
 270 The % TOC content presents moderate correlation with Al, Cu, Pb and Zn and negative correlation with Cr, Ni and the %  
 271 carbonates. Moreover, it shows poor correlation with Fe and Mn. Finally, the percentage of carbonates content presents  
 272 negative correlation with all metals.

#### 273 4.2 Enrichment Factors

274 The Enrichment Factors (EF) are used to distinguish between metals originating from anthropogenic activities and from  
 275 natural processes, assessing the degree of anthropogenic effect. Equation (1) was used for the calculations of EFs, where  $C_x$   
 276 is the concentration of the analyzed metal and  $C_{EN}$  is the concentration of the normalizing element. Al was used as the  
 277 reference element.

$$278 \text{EF} = (C_x/C_{EN})_{\text{sample}} / (C_x/C_{EN})_{\text{background}} \quad (1)$$

279 In Table 5, the categories of contamination according to the Enrichment Factor are presented (Diamantopoulou et al., 2019;  
 280 Sutherland, 2000). In general, EFs use concentrations normalized to Al to account for the heterogeneity of the samples due to  
 281 differences in texture and organic content (Gredilla et al., 2015).

282  
 283 **Table 5. The categories of infection according to the Enrichment Factor.**

EF	Contamination Degree
< 2	Depletion to minimal enrichment- no or minimal pollution
2 to 5	Moderate enrichment- moderate pollution
5 to 20	Significant enrichment- significant pollution
20 to 40	Very high enrichment- very strong pollution
>40	Extreme enrichment- extreme pollution

284  
 285 Table 6 shows the Enrichment Factors of the surface sediments (0-1 cm) of the study area that were calculated according to  
 286 the concentrations of heavy metals. The EFs were calculated at the fine fraction ( $f < 63\mu\text{m}$ ) of sediments of cores MOT13A,  
 287 MOT16, UN4. Most metals present minimal to moderate enrichment in almost all the cores analysed. Moderate enrichment  
 288 is found for Cr, Ni, Mn and Pb in core MOT13A, Mn in UN11, and finally for Pb in UN5 and MOT16.

289  
 290 **Table 6. Enrichment Factors of the surface sediments (0-1cm) of the study area. In cases of stations MOT13, MOT16, UN4, the**  
 291 **EFs were calculated at the fine surface sediment fraction ( $f < 63\mu\text{m}$ ).**

Core	EF Cr	EF Ni	EF Fe	EF Mn	EF Cu	EF Pb	EF Zn
MOT 13 A	3.09	2.07	1.92	2.07	1.94	2.24	2.14
MOT 16A	1.36	1.22	1.10	1.27	1.27	0.90	1.36
UN 5	1.20	1.28	1.17	1.64	1.42	2.32	1.74
MOT 16	1.28	1.14	1.05	1.33	1.61	3.71	1.60
UN6	0.98	0.98	0.99	1.43	1.36	1.73	1.57
UN 6A	1.00	0.99	1.01	1.23	1.15	1.09	1.39
UN 4	1.00	0.87	0.79	0.84	1.34	1.86	1.11
UN11	0.68	0.82	0.79	2.09	1.04	1.42	1.20

293



#### 294 4.3 Sediment Quality Guidelines

295 Sediment Quality Guidelines (SQG) of effect range low (ERL) and effect range median (ERM) are used to assess the level of  
296 toxicity of metals in the surface sediments. Metal concentrations below the ERL value, indicate that effects on biota are  
297 rarely observed. Concentrations above the ERL but below the ERM, occasionally affect the biota and concentrations above  
298 the ERM frequently affect the biota. The ERL and ERM guideline values for trace metals (ppm, dry wt) and percent  
299 incidence of biological effects in concentrations ranges defined by the two values are presented in Table 7 (Long et al.,  
300 1995).

301

302 **Table 7. ERL and ERM guideline values for trace metals (ppm, dry wt) and percent incidence of biological effects in concentration**  
303 **ranges defined by the two values.**  
304

Metal	ERL (mg kg <sup>-1</sup> )	ERM (mg kg <sup>-1</sup> )	Percent incidence of effects		
			<ERL	ERL-ERM	>ERM
Cr	81	370	2.9	21.1	95.0
Cu	34	270	9.4	29.1	83.7
Pb	46.7	218	8.0	35.8	90.2
Ni	20.9	51.6	1.9	16.7	16.9
Zn	150	410	6.1	47.0	69.8

305

306 In this study, the concentrations of heavy metals at the surface sediments were compared with the ERL and ERM criteria. In  
307 cases of cores MOT13A, MOT16, UN4, the concentrations of total sediment fraction (f < 1mm) were used for the  
308 comparison with ERL and ERM criteria. The concentrations of Cr in surface sediments of cores UN4, UN5, MOT16A, UN6,  
309 UN6A and UN11 are higher than the ERL value (81 mg Kg<sup>-1</sup>) but below the ERM value (370 mg Kg<sup>-1</sup>) (Hahladakis et al.,  
310 2012) and the values at surface sediments of MOT13A and MOT16 are higher than the ERM value. The concentrations of Ni  
311 at the surface sediments of the collected cores are higher than the ERM value (51.6 mg Kg<sup>-1</sup>) and as a result, they frequently  
312 affect the biota (Hahladakis et al., 2012).

313 The concentrations of Cu and Pb at surface sediments of stations MOT13A, MOT16A, UN4, UN5, MOT16 and UN6A, are  
314 below the ERL values (34 mg Kg<sup>-1</sup> for Cu and 46.7 mg Kg<sup>-1</sup> for Pb), which indicates that effects on biota are rarely  
315 observed. On the other hand, the concentrations at surface sediments of cores UN6 and UN11 are higher than the ERL values  
316 but below the ERM values (270 mg Kg<sup>-1</sup> for Cu and 218 mg Kg<sup>-1</sup> for Pb), which means that they can occasionally affect the  
317 biota (Hahladakis et al., 2012). The concentrations of Zn are below the ERL (150 mg Kg<sup>-1</sup>) value and the ERM value (410  
318 mg Kg<sup>-1</sup>), which indicates that effects on biota are rarely observed (Hahladakis et al., 2012).

#### 319 4.4 Mean effects range medium quotients

320 The mean effects range medium quotient (mERMq) is an index that is used to evaluate the possible biological effects of the  
321 coupled toxicity of all heavy metals in the surface sediments (Gredilla et al., 2015). Briefly, mERMq's were calculated by  
322 dividing the average concentration of each metal at the top 9cm, by its respective ERM (effects range median), to obtain the  
323 corresponding sediment quality guideline quotient (ERMq). Following this, mERMq's for each core were obtained as the  
324 average of ERMqs previously calculated. ERMqs indicates the pollutant concentration above which effects are expected to  
325 be frequent and have been only defined for very toxic elements (Gredilla et al., 2015).

326 In this study, Cr, Ni, Cu, Pb and Zn were considered in our calculations and the results are depicted in Table 8. In cases of  
327 cores MOT13A, MOT16, UN4, the concentrations of total sediment fraction (f < 1mm) were used for the calculation of  
328 mERMq. Values of mERMq in the ranges of 0.0-0.1, 0.1-0.5, 0.5-1.5 and >1.5 correspond to the following probabilities of  
329 toxicity: 9 % (non-toxic), 21 % (slightly toxic), 49 % (moderately toxic) and 76 % (highly toxic), respectively (Gredilla et  
330 al., 2015). The mERMq values obtained for the sediments varied from 0.62 to 2.00, which means that the sediments are  
331 moderately or highly toxic.



332 The concentrations of Cr, Ni, Cu, Pb, Zn in sediments of cores MOT13A, UN5, UN6, UN6A, UN4 and UN11 are  
333 moderately toxic and in sediments of MOT16A and MOT16 highly toxic. The concentrations of Cu, Pb, Zn in sediments of  
334 cores MOT13A, MOT16A, MOT16, UN4 are non-toxic, with mERMq range 0.08-0.10 and those in sediments of UN5,  
335 UN6, UN6A, UN11 are slightly toxic, with mERMq range 0.16-0.21.

336

337 **Table 8. MERMqs values calculated for the surface sediments (0-9 cm) of the collected cores of West Saronikos Gulf, by dividing**  
338 **the average concentration ( $\text{mg Kg}^{-1}$ ) of each metal (Cr, Ni, Cu, Pb, Zn) by its respective ERM ( $\text{mg Kg}^{-1}$ ). In cases of cores**  
339 **MOT13A, MOT16, UN4, the concentrations of total sediment fraction ( $f < 1\text{mm}$ ) were used for the calculation of mERMq.**  
340

Core	mERMq (average)	toxicity of sediments
MOT13A	1.46	Moderately toxic
MOT16A	1.69	Highly toxic
UN5	1.46	Moderately toxic
MOT16	2.00	Highly toxic
UN6	1.21	Moderately toxic
UN6A	0.95	Moderately toxic
UN4	0.62	Moderately toxic
UN11	1.09	Moderately toxic

341

#### 342 4.5 Evolution of marine pollution

343 The total concentrations of eight heavy metals in the surface sediments were compared with those of a similar study ten  
344 years ago (Paraskevopoulou, 2009). In cases of cores MOT13A, MOT16, UN4, the concentrations of total sediment fraction  
345 ( $f < 1\text{mm}$ ) were used and the results are depicted in Fig.6. The levels of Cr, Ni, Mn at most sediments, are decreased in 2017,  
346 compared to the study of 2007. On the other hand, the levels of Pb and Cu are increased in 2017, compared to the study of  
347 2007. Moreover, the levels of Zn, at most sediments, are decreased in 2017 compared to the study of 2007.

348

349

350

351

352

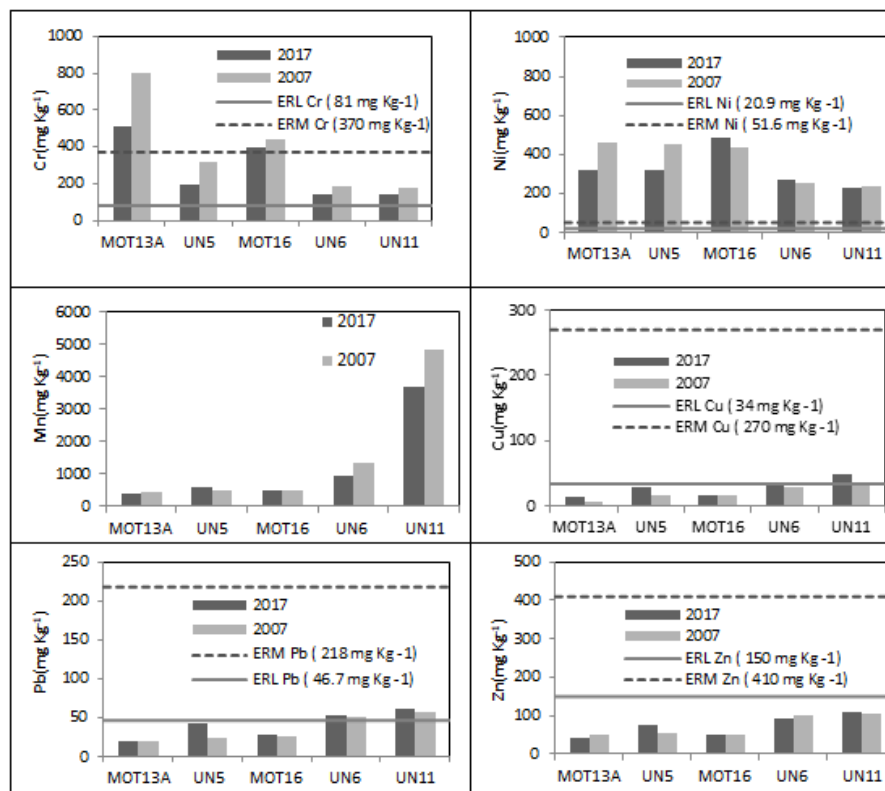
353

354

355

356

357



358

359 **Figure 6:** Levels of heavy metals in surface sediments of 2017 and 2007 and sediment quality guidelines. In cases of coarse  
360 sediments of stations MOT13A, MOT16, UN4, the concentrations of total sediment fraction ( $f < 1\text{mm}$ ) were used.  
361

#### 362 4.6 Comparison of metal concentrations in West Saronikos Gulf with other areas of Saronikos Gulf

363 The concentrations of heavy metals in surface sediments of West Saronikos Gulf are compared with those measured at  
364 Elefsis Bay (EB), Inner Saronikos Gulf (ISG) and Outer Saronikos Gulf (OSG) from the sampling of October 2017  
365 (Panagopoulou, 2018; Vrettou, 2019; Xarlis, 2018). Figure 7 shows the location of sampling stations.

366 The station at Elefsis Bay with depth of 25 m locates near the Elefsis Port and station at Inner Saronikos Gulf with depth of  
367 75 m near the Psittalia WWTP outfall. Moreover, there are two stations at Outer Saronikos Gulf. The first one, with depth of  
368 85 m, locates near Vouliagmeni and the last one, with depth of 189 m, northwest of Sounio. The silt and clay fraction ( $f <$   
369  $63\mu\text{m}$ ) of surface sediments northwest of Sounio and near the Psittalia is higher than the sand fraction ( $63\mu\text{m} < f < 1\text{mm}$ ).

370 The sand fraction of the surface sediment near Vouliagmeni is higher than the silt and clay and similar to silt and clay of  
371 surface sediment of Elefsis Gulf. The total metal contents were extracted via complete dissolution of sediment samples with  
372 an acid mixture of  $\text{HNO}_3\text{-HClO}_4\text{-HF}$  (ISO-14869-1:2000) (Peña-Icart et al., 2011).



373  
 374 **Figure 7: Map of Saronikos Gulf and the location of sediment sampling stations (© Google Earth 2019). The station at Elefsis Bay**  
 375 **locates near the Elefsis Port and station at Inner Saronikos Gulf near the Psittalia WWTP outfall. Moreover, there are two**  
 376 **stations at Outer Saronikos Gulf. The first one, locates near Vouliagmeni and the last one, northwest of Sounio.**

377  
 378 The levels of Al of West Saronikos are comparable with those at the other areas and the low concentration of Al at station  
 379 near Vouliagmeni can be explained by the coarse surface sediment. The concentrations of Ni are decreased from the  
 380 northwest to the southeast part of Saronikos Gulf. High levels of Ni at the northwest area can be attributed to its geological  
 381 origin (Kelepeptsis et al., 2001). The levels of Fe at West Saronikos are comparable with those at the other sediments. The  
 382 low content of Fe at station near Vouliagmeni may be attributed to its coarse sediment. The maximum values of Al, Fe and  
 383 Mn at station UN11 can be attributed to the fine surface sediment and the hypoxic conditions at waters of West Saronikos  
 384 deeper than 200m. Generally, the levels of Mn at West Saronikos are higher than those measured at Psittalia, Elefsis Gulf  
 385 and station near Vouliagmeni. The highest concentrations of Mn are observed at the deepest stations (UN6 and UN11 of  
 386 West Saronikos and station northwest of Sounio).

387 The levels of Cu, Pb, Zn at surface sediments of Psittalia and Elefsis Gulf are higher than those observed at the other  
 388 sediments, which can be explained by the numerous pollution sources in the marine environment and along the coast of Inner  
 389 Saronikos Gulf and Elefsis Bay (Paraskevopoulou et al., 2014). Especially the concentrations of Cu at the northwest part are  
 390 comparable with those at Outer Saronikos Gulf but lower than those at the deep station UN11 and the concentrations of Pb at  
 391 West Saronikos are comparable with those at Outer Saronikos. The levels of Zn at the northwest part are higher than those  
 392 observed near Vouliagmeni, but lower than those at station UN11 and at the northwest area of Sounio. The results are  
 393 depicted at Table 9. In cases of coarse surface sediments, the concentrations at total sediment fraction ( $f < 1$  mm) were used.

394  
 395 **Table 9. Comparison of heavy metals concentrations in mg Kg<sup>-1</sup> measured in this study with those in other areas of Saronikos.**

Station	Al	Ni	Fe	Mn	Cu	Pb	Zn	References
MOT13A	5697	344	20740	422	13.5	20.0	44.1	Present work
MOT16A	27009	375	23315	578	22.6	20.4	48.3	Present work
UN5	32705	305	25534	635	27.4	42.7	74.5	Present work
MOT16	16050	484	31191	503	16.9	30.3	52.1	Present work
UN6	43264	253	27301	954	36.7	52.9	92.1	Present work
UN6A	39314	187	21838	570	26.3	38.4	73.8	Present work
UN4	22702	123	16682	270	17.5	24.5	43.6	Present work
UN11	54626	230	32177	3925	49.7	63.9	110	Present work
Psittalia	26780	83.2	20623	239	103	102	251	Panagopoulou, 2018; Xarlis, 2018
Elefsis Gulf	44853	109	30499	394	132	141	368	Panagopoulou, 2018; Xarlis, 2018
Vouliagmeni	4424	13.4	6407	243	10.5	40.1	27.4	Vrettou, 2019
NWSounio	44902	114	27139	958	30.7	64.1	141	Vrettou, 2019

396  
 397  
 398





## 399 5 Conclusions

400 The heavy metal pollution of West Saronikos Gulf has not been sufficiently studied, despite the scientific interest of this  
 401 area, in contrast to the numerous studies of the eastern coast. The distribution of metals in the sediment samples of West  
 402 Saronikos indicates that the area is enriched in metals from both geological and anthropogenic origins. The concentrations of  
 403 all metals (Al, Mn, Cr, Ni, Cu, Pb, Zn) of fine sediments are higher than those measured in coarse sediments. The cores are  
 404 fairly homogeneous, in terms of carbonates and the down-core variability of % TOC, is characterized by high surficial values  
 405 that decrease with depth.

406 The Cr and Ni concentrations at the northwest part of the study area are higher than those measured at the southwest area and  
 407 their values are very stable with depth of most sediment cores, which can be explained by the ophiolite background  
 408 (Kelepertsis et al., 2001). Al, Fe and Mn are increased from the northeast to the southwest part of the study area. The  
 409 concentrations of Al and Fe are increased with depth of most cores, while the values of Mn are decreased with depth.  
 410 Generally, concentrations of Fe and Mn at surface sediments are affected by oxic and hypoxic conditions.

411 The horizontal distributions of Cu, Pb and Zn present a constant decrease over depth along most cores, which can be  
 412 attributed to their anthropogenic origin. Moreover, their levels at most sediments are higher than those measured ten years  
 413 ago. Finally, the Cu, Pb, Zn concentrations in West Saronikos Gulf surface sediments are comparable with those at Outer  
 414 Saronikos Gulf and lower than those from Inner Saronikos Gulf and Elefsis Bay, which can be attributed to the smaller  
 415 industrial zone of the west coast in comparison to the numerous anthropogenic activities at the east coast.

416 The concentrations of metals that are measured higher than the ERL values and the indication for moderately or highly toxic  
 417 sediments by the calculation of mERMq signify that more research is required, in order to investigate probable effects on the  
 418 marine ecosystem. Continuous monitoring, updating of the results of the present work, metal speciation and study of  
 419 bioaccumulation should be conducted, to assess the impacts of heavy metal pollution on the marine environment of West  
 420 Saronikos Gulf.

## 421 6 Appendices

### 422 Appendix A

423

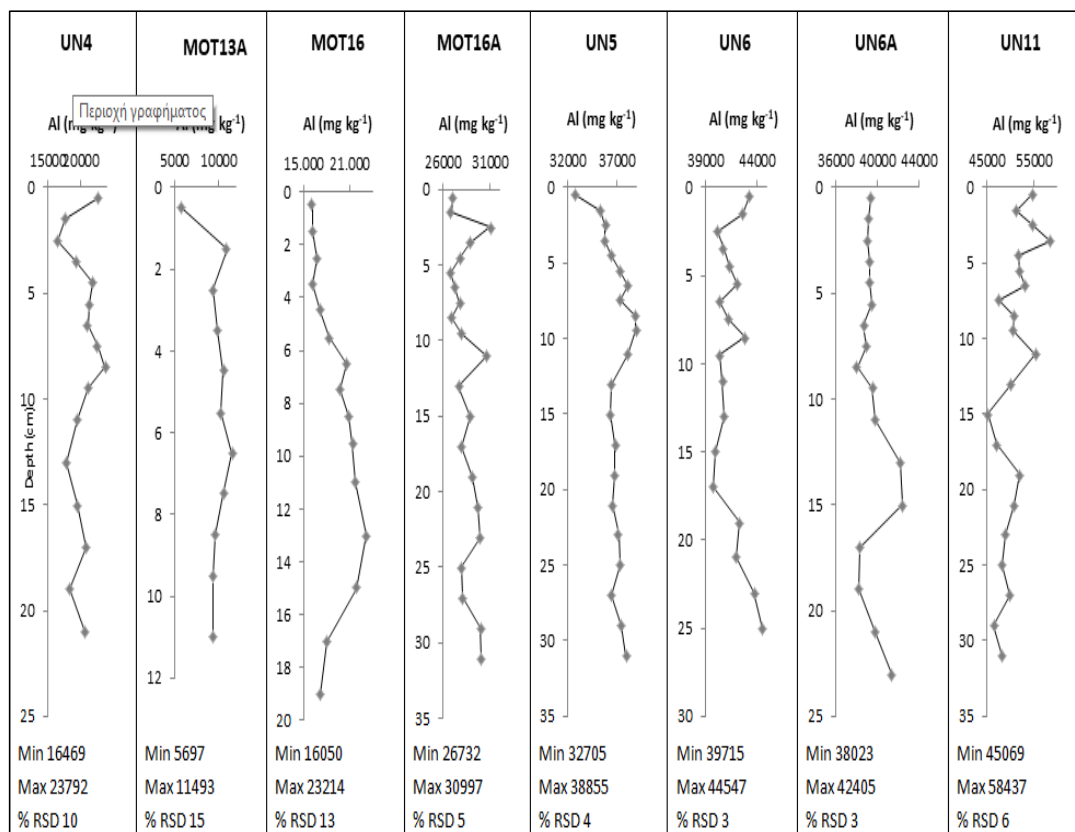
424 **Table A1. The ratios of eight heavy metals to Al in surface sediments and sediments of the depth of the collected cores. In cases of**  
 425 **coarse-sediment cores MOT13A, MOT16, UN4, the ratios in fine sediment fraction ( $f < 63 \mu\text{m}$ ) are measured.**

426

Core	Layer (cm)	Cr $10^4 \text{ Al}^{-1}$	Ni $10^4 \text{ Al}^{-1}$	Fe $\text{Al}^{-1}$	Mn $10^4 \text{ Al}^{-1}$	Cu $10^4 \text{ Al}^{-1}$	Pb $10^4 \text{ Al}^{-1}$	Zn $10^4 \text{ Al}^{-1}$
MOT 13 A	0-1	616	389	1.99	451	17.3	24.7	46.9
	10-12	277	261	1.44	303	12.4	15.4	30.4
MOT 16A	0-1	104	139	0.86	214	8.35	7.55	17.9
	30-32	85.0	127	0.87	187	7.35	9.35	14.7
UN 5	0-1	61.0	93.1	0.78	194	8.39	13.1	22.8
	30-32	58.9	84.5	0.77	137	6.85	6.52	15.2
MOT 16	0-1	170	174	1.19	244	10.4	12.9	24.8
	18-20	146	168	1.25	203	7.11	3.81	17.0
UN6	0-1	32.7	58.4	0.63	220	8.48	12.2	21.3
	24-26	34.2	61.6	0.66	159	6.41	7.29	14.0
UN 6A	0-1	37.0	47.5	0.56	145	6.7	9.76	18.8
	22-24	39.0	50.6	0.58	124	6.14	9.38	14.2
UN 4	0-1	38.6	47.4	0.46	104	6.9	7.63	15.2
	20-22	35.7	50.5	0.54	115	4.75	3.80	12.7
UN11	0-1	26.1	42.0	0.59	719	9.1	11.7	20.2
	30-32	33.8	45.1	0.66	303	7.75	7.29	14.8

427

428

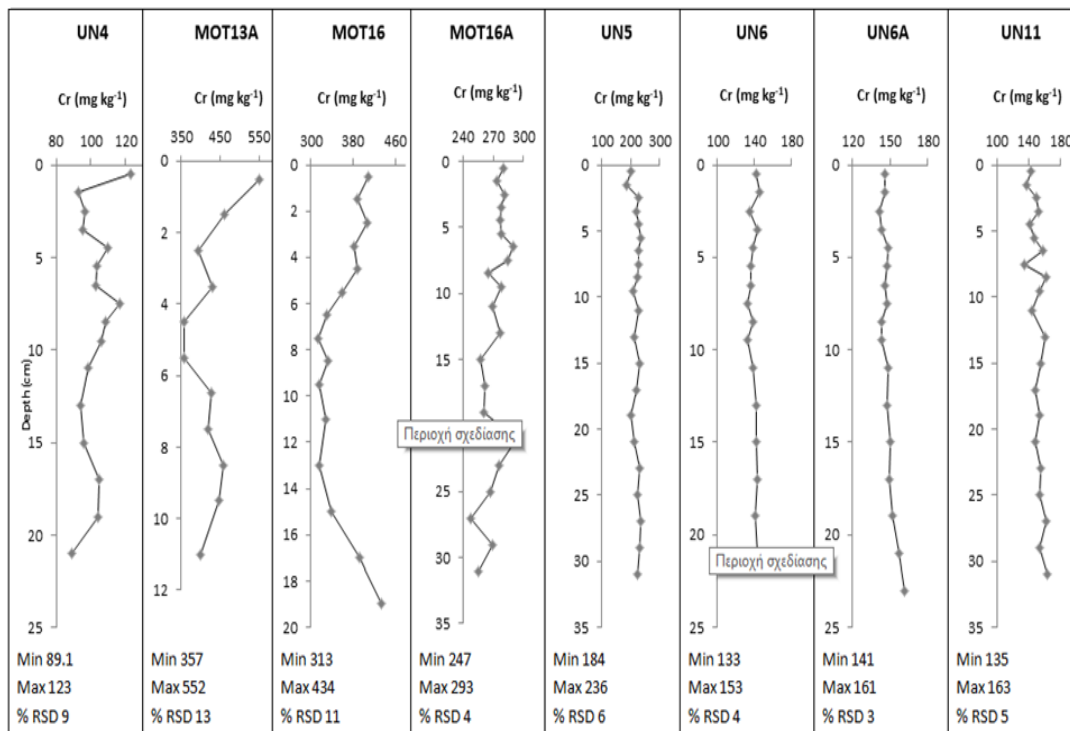


429

430

431

**Figure A1:** Vertical distributions of Al in mg kg<sup>-1</sup> in sediment cores. The concentrations in coarse cores MOT13A, MOT16, UN4 refer to the total sediment fraction (f < 1 mm).

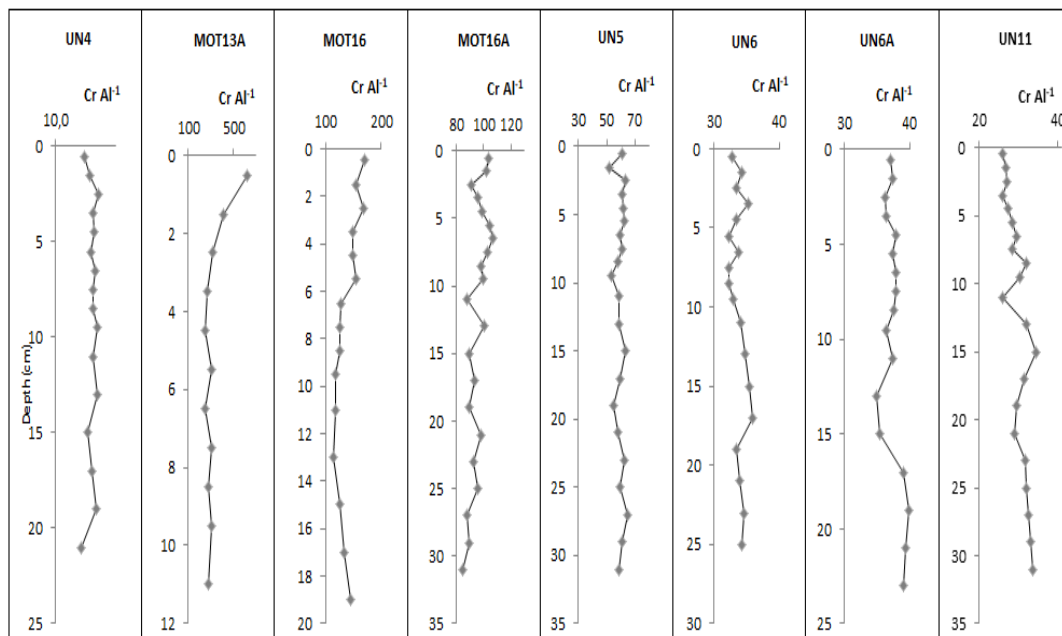


432

433

434

Figure A2: Vertical distributions of Cr in mg kg<sup>-1</sup> in sediment cores. The concentrations in coarse cores MOT13A, MOT16, UN4 refer to the total sediment fraction (f < 1 mm).

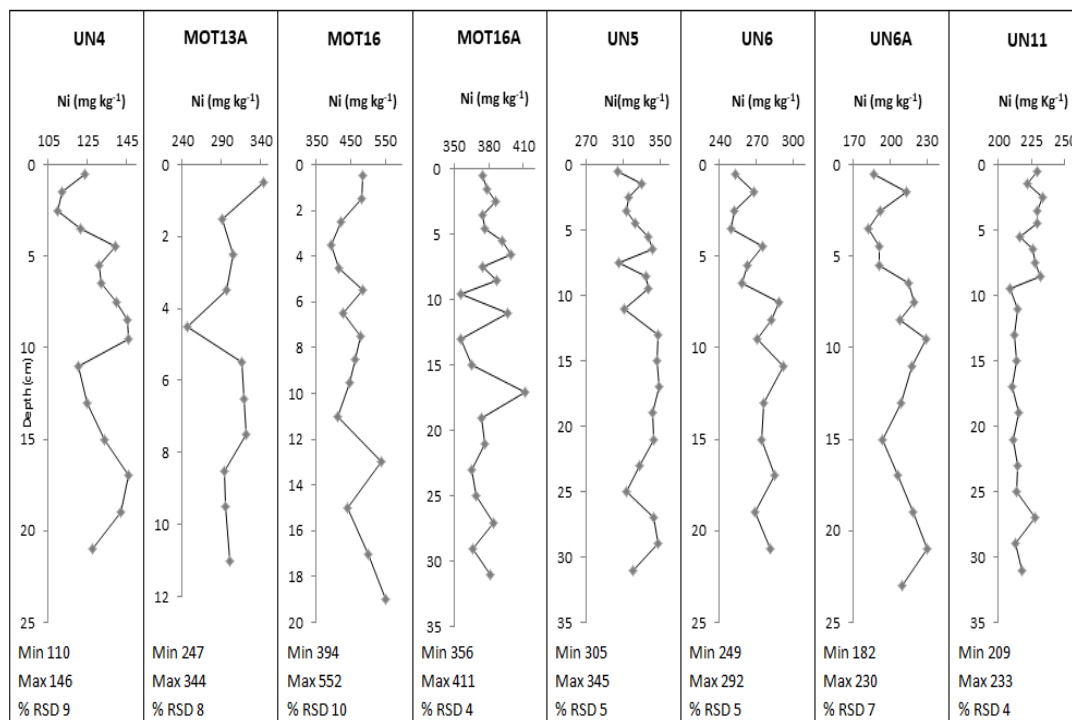


435

436

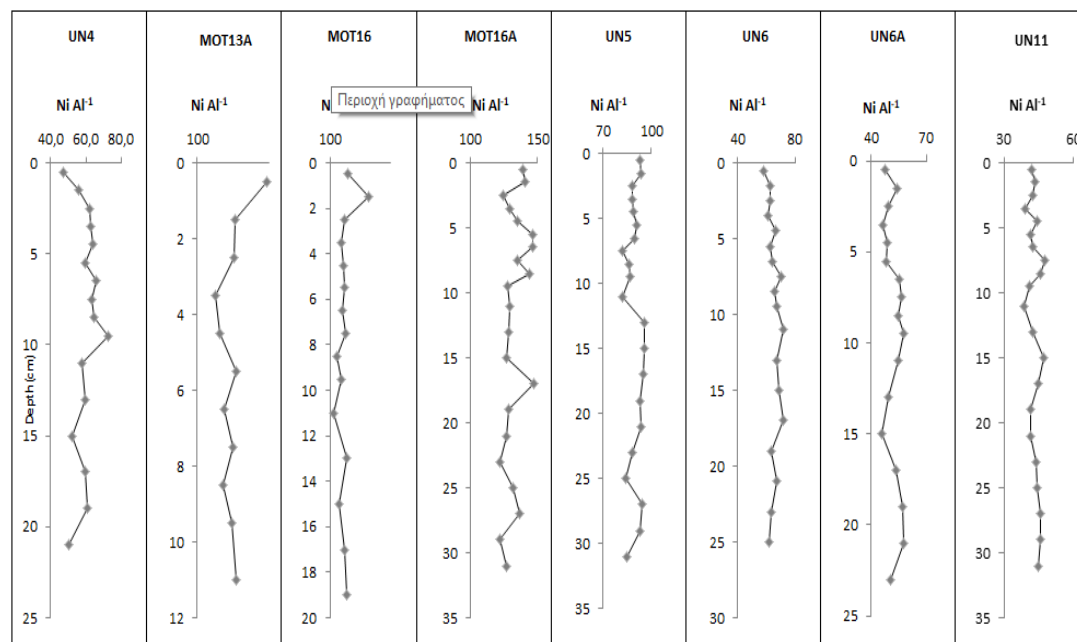
437

Figure A3: Vertical distributions of Cr Al<sup>-1</sup> (10<sup>4</sup>) in sediment cores. The ratios in coarse cores MOT13A, MOT16, UN4 are calculated at the fine sediment fraction (f < 63 μm).



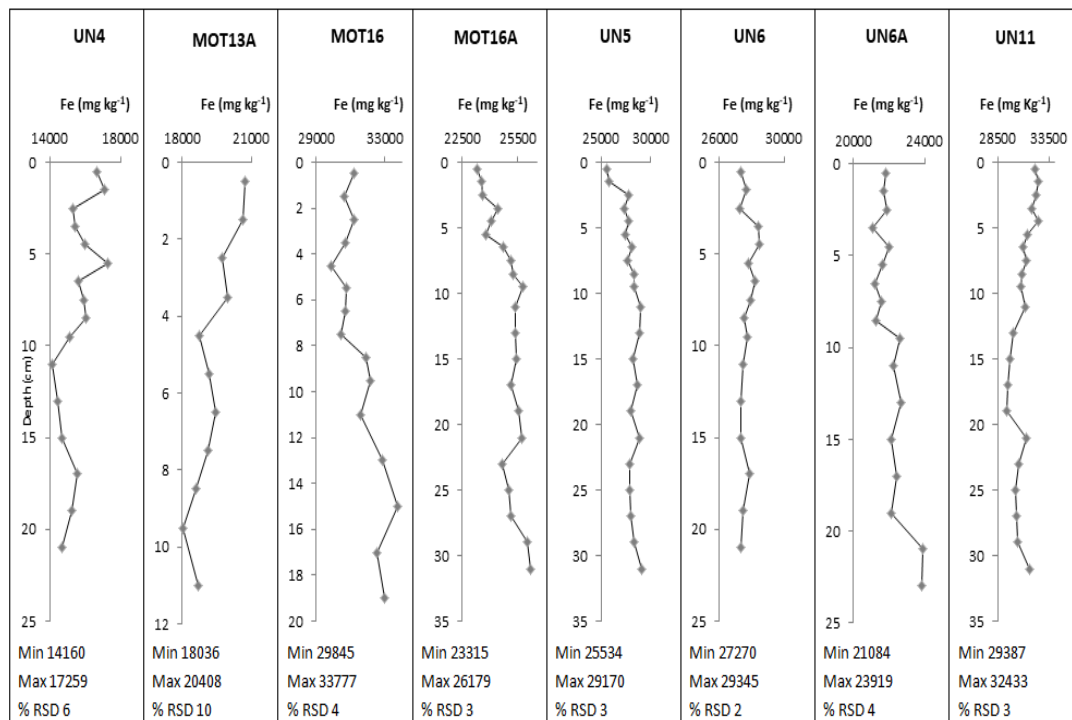
438

439 **Figure A4: Vertical distributions of Ni in mg kg<sup>-1</sup> in sediment cores. The concentrations in coarse cores MOT13A, MOT16, UN4**  
 440 **refer to the total sediment fraction (f < 1 mm).**



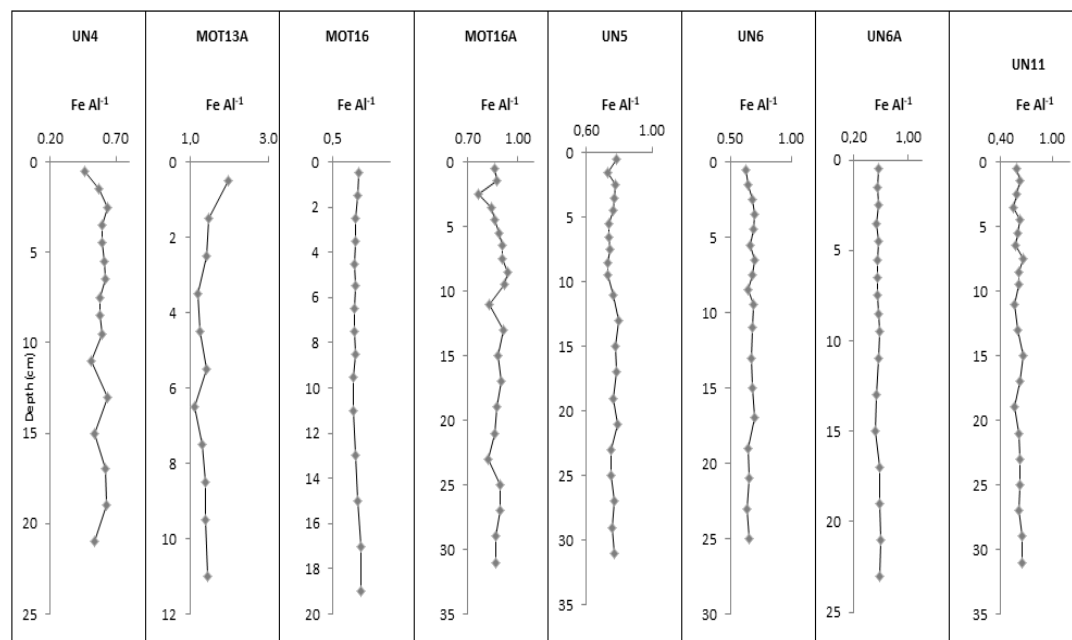
441

442 **Figure A5: Vertical distributions of Ni Al<sup>-1</sup> (10<sup>4</sup>) in sediment cores. The ratios in coarse cores MOT13A, MOT16, UN4**  
 443 **are calculated at the fine sediment fraction (f < 63 μm).**



444

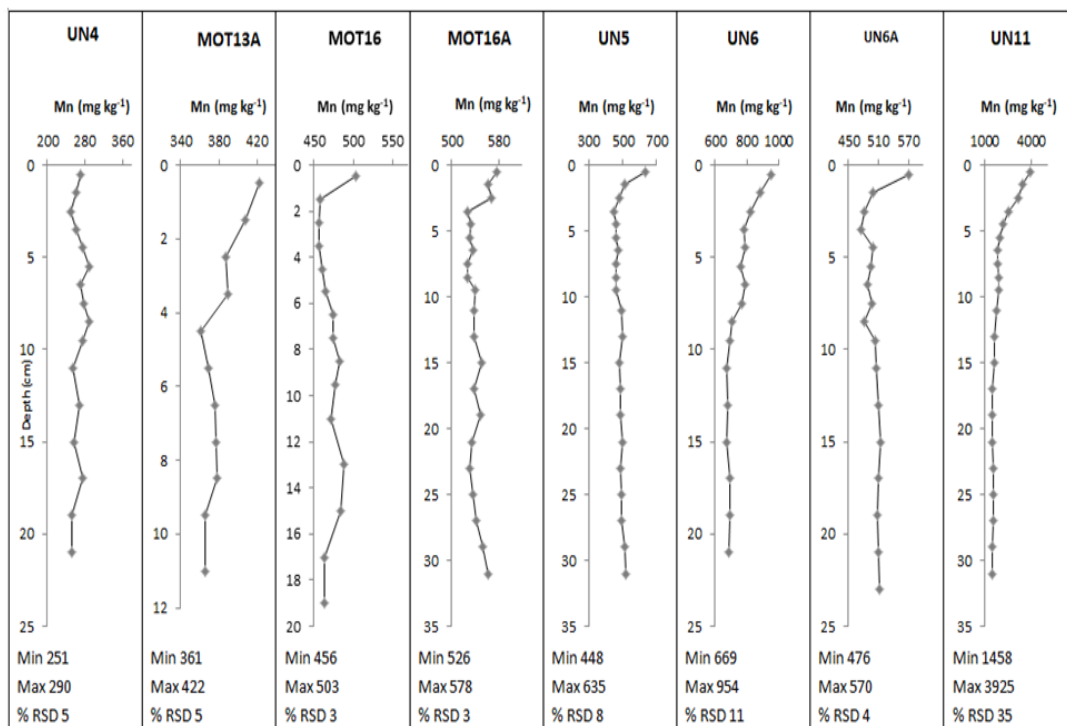
445 **Figure A6: Vertical distributions of Fe in mg kg<sup>-1</sup> in sediment cores. The concentrations in coarse cores MOT13A, MOT16, UN4**  
 446 **refer to the total sediment fraction (f < 1 mm).**



447

448 **Figure A7: Vertical distributions of Fe Al<sup>-1</sup> in sediment cores. The ratios in coarse cores MOT13A, MOT16, UN4 are calculated at**  
 449 **the fine sediment fraction (f < 63 μm).**

450

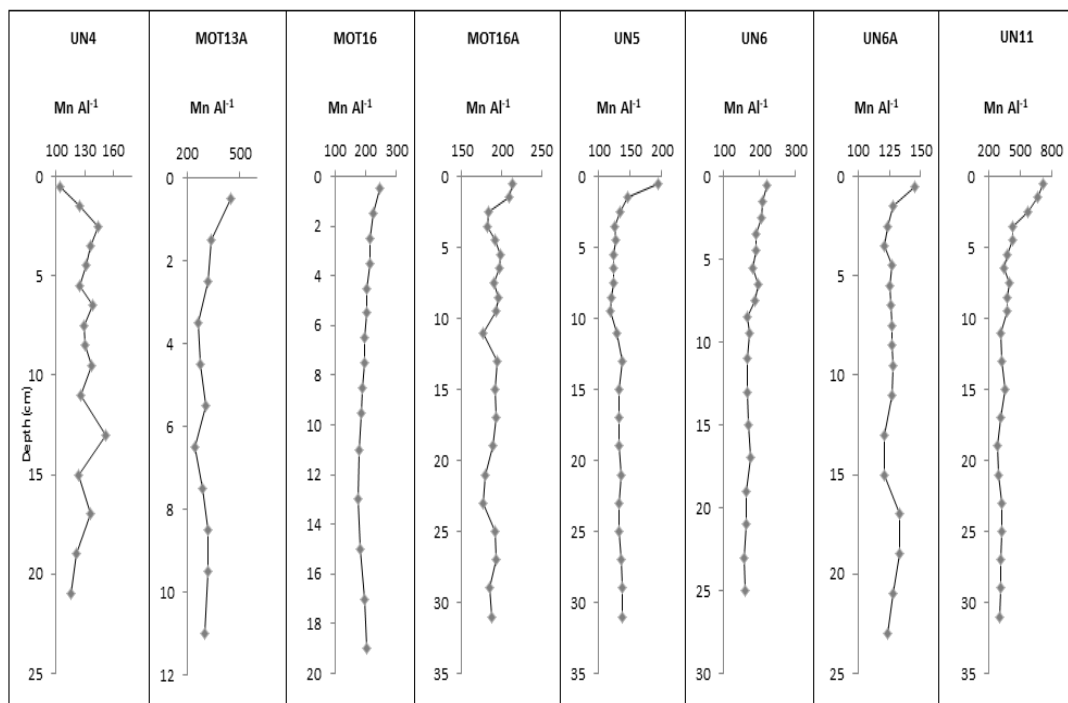


451

452

453

Figure A8: Vertical distributions of Mn in mg kg<sup>-1</sup> in sediment cores. The concentrations in coarse cores MOT13A, MOT16, UN4 refer to the total sediment fraction (f < 1 mm).



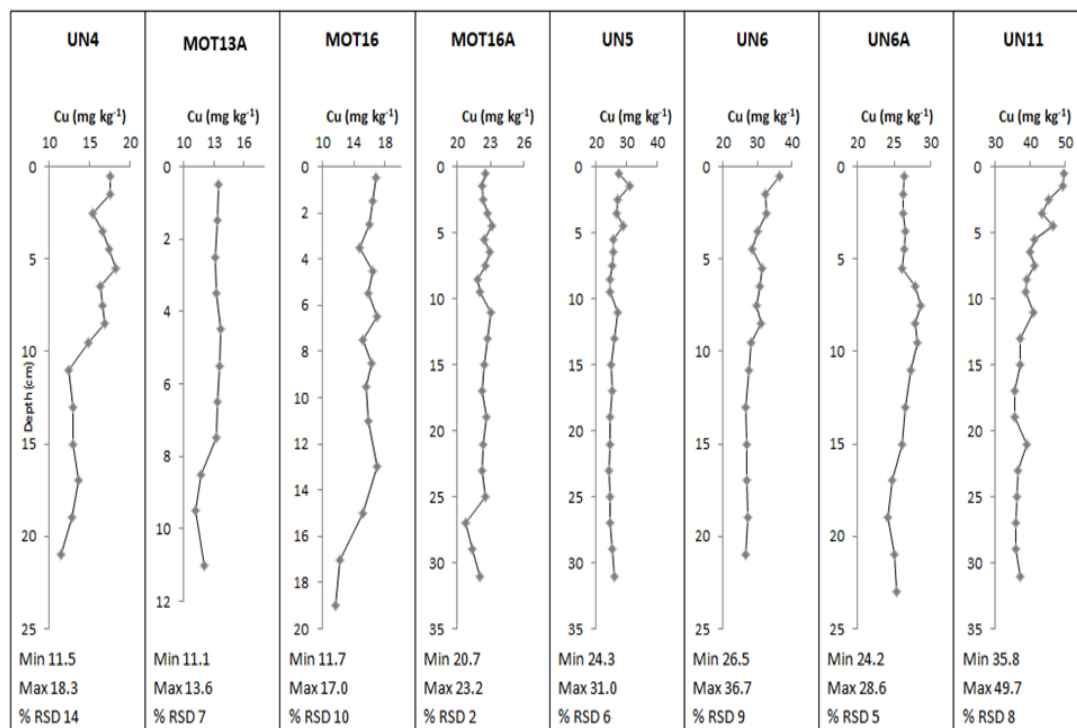
454

455

456

Figure A9: Vertical distributions of Mn Al<sup>-1</sup> (10<sup>4</sup>) in sediment cores. The ratios in coarse cores MOT13A, MOT16, UN4 are calculated at the fine sediment fraction (f < 63 μm).



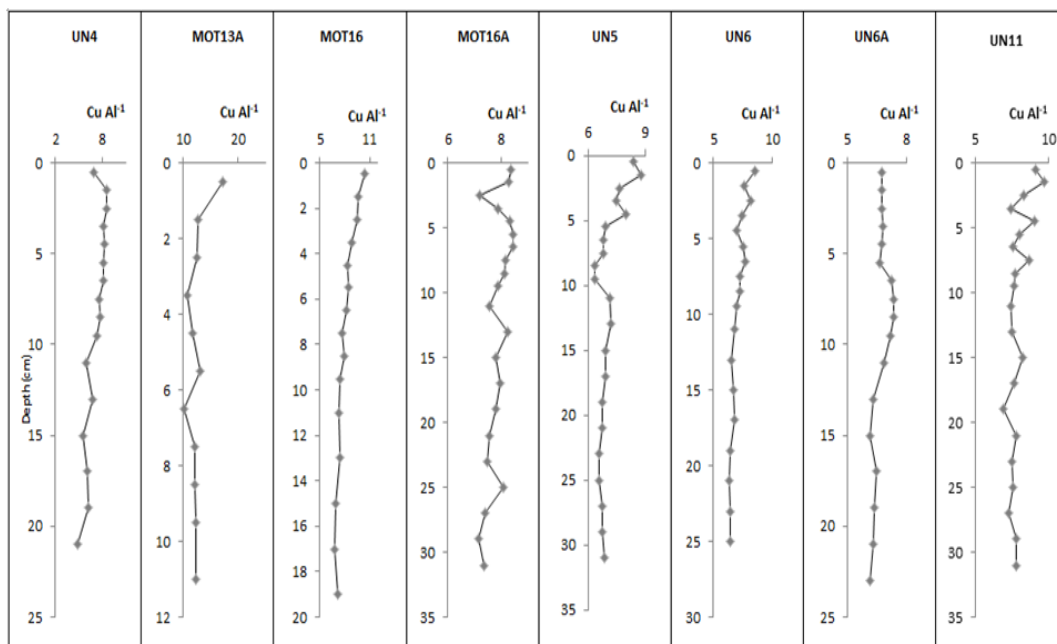


457

458

459

Figure A10 : Vertical distributions of Cu in mg kg<sup>-1</sup> in sediment cores. The concentrations in coarse cores MOT13A, MOT16, UN4 refer to the total sediment fraction ( $f < 1$  mm).



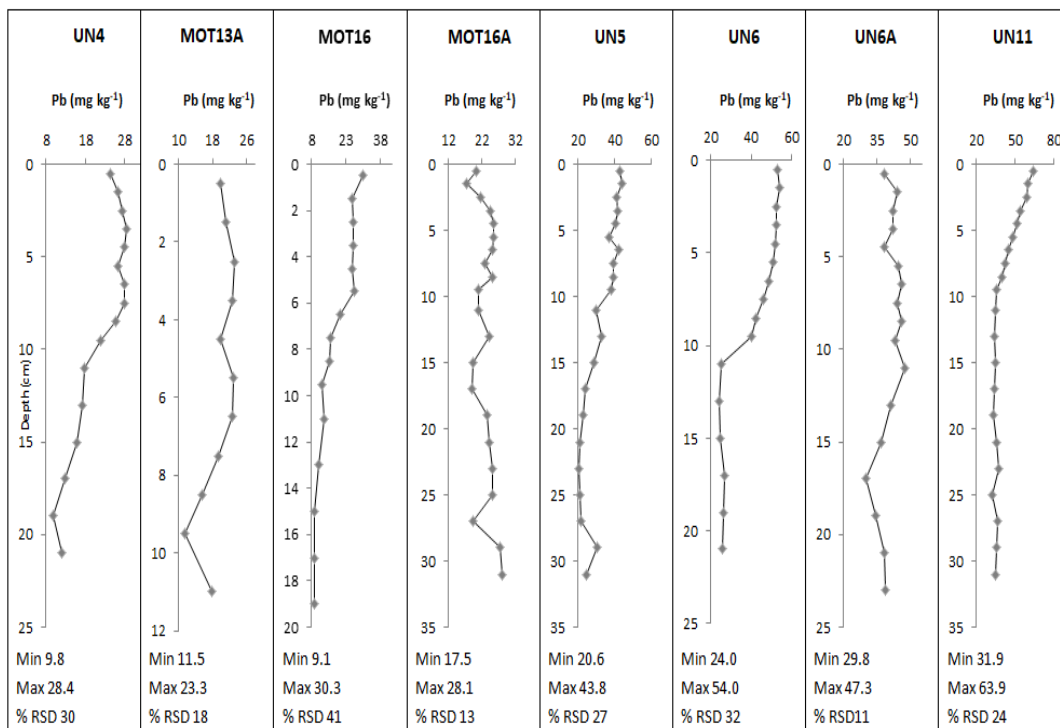
460

461

462

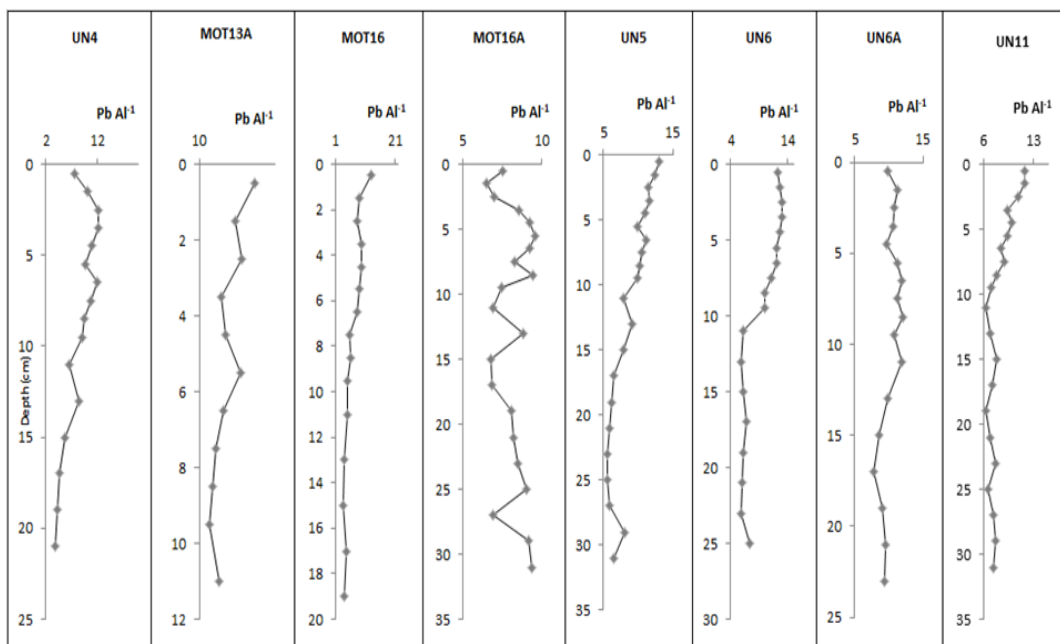
463

Figure A11: Vertical distributions of Cu Al<sup>-1</sup> (10<sup>4</sup>) in sediment cores. The ratios in coarse cores MOT13A, MOT16, UN4 are calculated at the fine sediment fraction ( $f < 63$   $\mu$ m).



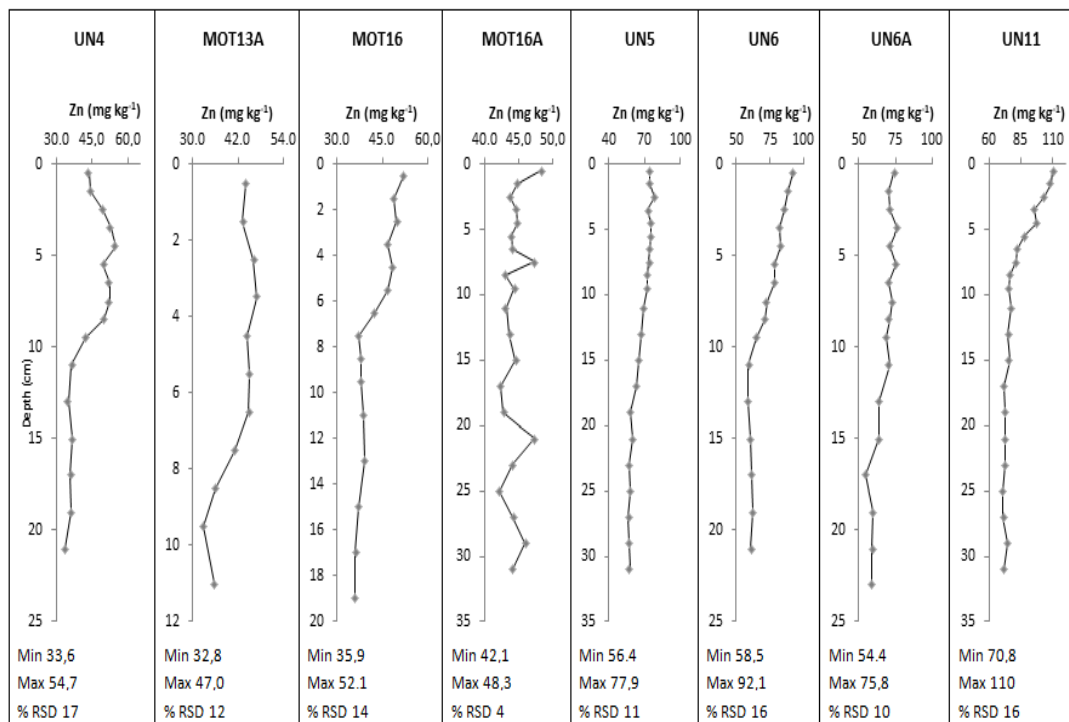
464

465 **Figure A12: Vertical distributions of Pb in mg kg<sup>-1</sup> in sediment cores. The concentrations in coarse cores MOT13A, MOT16, UN4**  
 466 **refer to the total sediment fraction (f < 1 mm).**



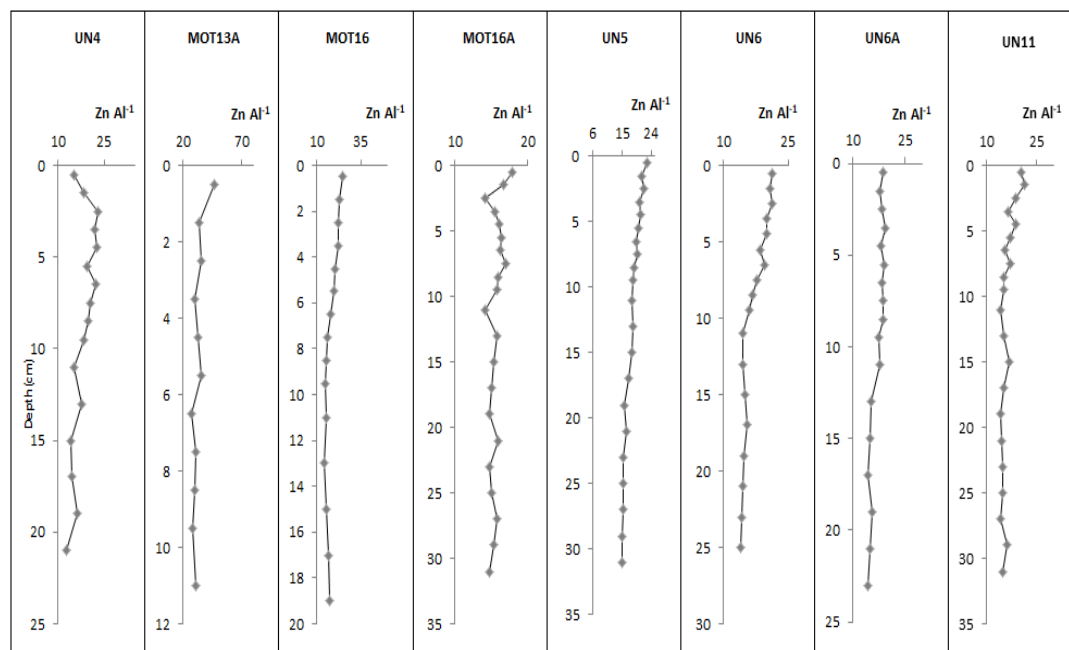
467

468 **Figure A13: Vertical distributions of Pb Al<sup>-1</sup> (10<sup>4</sup>) in sediment cores. The ratios in coarse cores MOT13A, MOT16, UN4 are**  
 469 **calculated at the fine sediment fraction (f < 63 μm).**



470

471 **Figure A14: Vertical distributions of Zn in mg kg<sup>-1</sup> in sediment cores. The concentrations in coarse cores MOT13A, MOT16, UN4**  
 472 **refer to the total sediment fraction (f < 1 mm).**



473

474 **Figure A15: Vertical distributions of Zn Al<sup>-1</sup> (10<sup>4</sup>) in sediment cores. The ratios in coarse cores MOT13A, MOT16, UN4 are**  
 475 **calculated at the fine sediment fraction (f < 63 μm).**



476 **Table A2. Spearman's correlation coefficient matrix for Al (mg Kg<sup>-1</sup>), Cr (mg Kg<sup>-1</sup>), Ni (mg Kg<sup>-1</sup>), Fe (mg Kg<sup>-1</sup>), Mn (mg Kg<sup>-1</sup>), Cu**  
 477 **(mg Kg<sup>-1</sup>), Pb (mg Kg<sup>-1</sup>), Zn (mg Kg<sup>-1</sup>), TOC (% Total Organic Carbon), carbonates (% CaCO<sub>3</sub>) (N=140 sediment samples).**

478

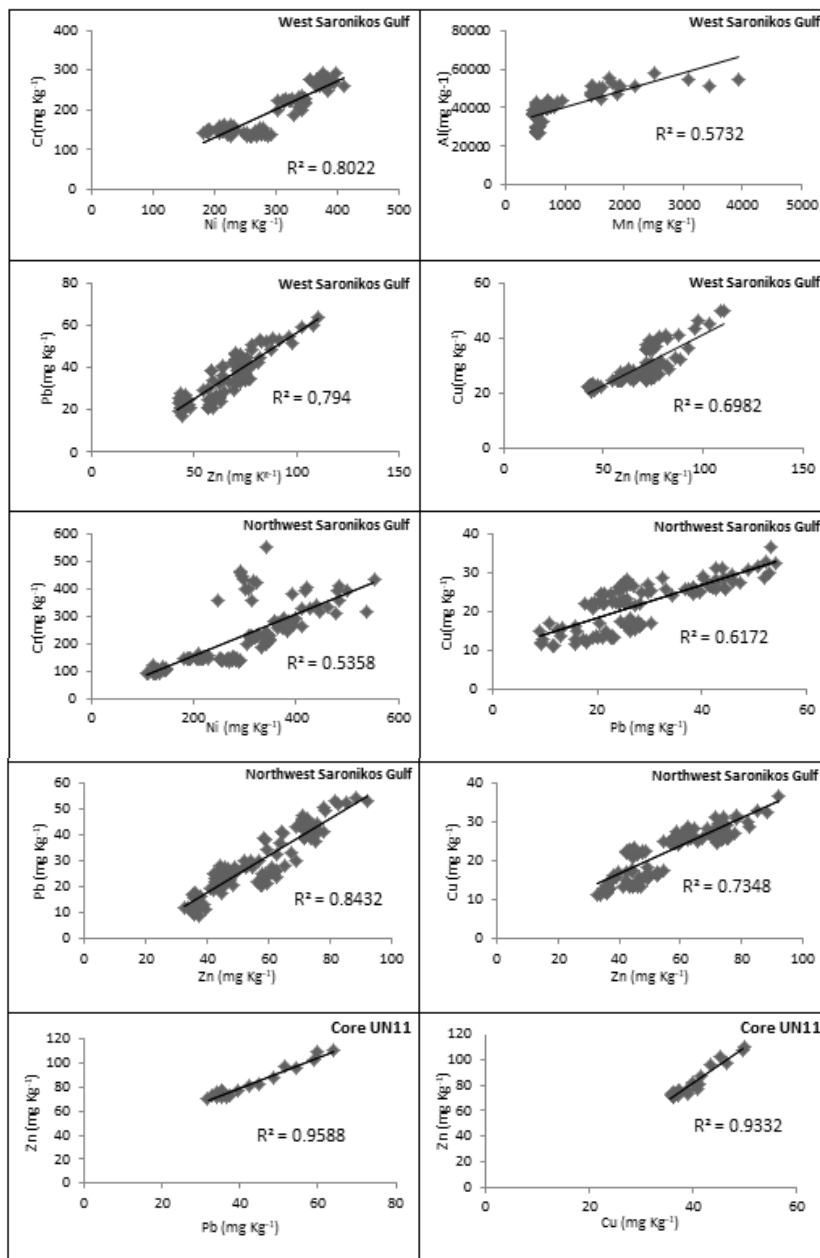
Correlations										
Spearman's rho	Al	Cr	Ni	Fe	Mn	Cu	Pb	Zn	TOC	% CaCO <sub>3</sub>
Al	1.000									
Cr	-0.521**	1.000								
Ni	-0.453**	0.841**	1.000							
Fe	0.624**	0.081	0.179*	1.000						
Mn	0.735**	-0.108	0.029	0.694**	1.000					
Cu	0.924**	-0.419**	-0.342**	0.633**	0.746**	1.000				
Pb	0.676**	-0.440**	-0.433**	0.244**	0.397**	0.779**	1.000			
Zn	0.790**	-0.452**	-0.441**	0.459**	0.479**	0.882**	0.894**	1.000		
TOC	0.244**	-0.198*	-0.272**	0.096	0.155	0.351**	0.428**	0.483**	1.000	
% CaCO <sub>3</sub>	-0.472**	-0.215*	-0.222**	-0.766**	-0.597**	-0.566**	-0.358**	-0.516**	-0.282**	1.000

\*\* . Correlation is significant at the 0.01 level (2-tailed).

\* . Correlation is significant at the 0.05 level (2-tailed).



479



480  
481  
482  
483  
484  
485  
486  
487  
488  
489  
490  
491  
492  
493  
494  
495  
496  
497  
498  
499  
500  
501

Figure A16: Correlations of heavy metals for the core samples of West Saronikos Gulf.



502 **7 Data availability**

503 Datasets and their sources are fully detailed in the manuscript.

504

505 **8 Team list**

506 Not applicable.

507

508 **9 Author contribution**

509 Georgia Filippi and Vasiliki Paraskevopoulou conducted the chemical analyses in the Laboratory of Environmental  
510 Chemistry of the National and Kapodistrian University of Athens. Georgia Filippi wrote the paper, with contributions and  
511 reviews from all co-authors. Manos Dassenakis was the supervisor of the laboratory work and this article.

512

513 **10 Competing interests**

514 The authors declare that they have no conflict of interest.

515

516 **11 Special issue statement**

517 The statement on a corresponding special issue will be included by Copernicus, if applicable.

518

519 **12 Acknowledgements**

520 We are grateful to the Hellenic Center for Marine Research (HCMR) and our colleagues Prof. S. Poulos, Dr Aik. Karditsa,  
521 and Dr F. Botsou for the assistance during the sampling. The research was funded by the European Union (European Social  
522 Fund) and National Funds (Hellenic General Secretariat for Research and Technology) in the framework of the project  
523 ARISTEIA I, 640 “Integrated Study of Trace Metals Biogeochemistry in the Coastal Marine Environment”, within the  
524 “Lifelong Learning Programme”. This project gave us the opportunity to reach the heavy metal pollution of West Saronikos  
525 Gulf. This paper summarizes the results of this study.

526

527 **13 References**

528

529 Barjy, M., Maanan, M., Maanan, M., Salhi, F., Tnoumi, A., and Zourarah, B.: Contamination and environmental risk  
530 assessment of heavy metals in marine sediments from Tahaddart estuary (NW of Morocco), *Hum. And Ec. R. Assess.*, 26,  
531 71-86, <https://doi.org/10.1080/10807039.2018.1495056>, 2020.

532

533 Bigus, P., Tobiszewski, M., and Namiesnik, J.: Historical records of organic pollutants in sediment cores, *Mar. Poll. Bull.*,  
534 78, 26-42, [10.1016/j.marpolbul.2013.11.008](https://doi.org/10.1016/j.marpolbul.2013.11.008), 2014.

535

536 Diamantopoulou, A., Kalavrouziotis, I.K., and Varnavas, S.P.: Geochemical investigations regarding the variability of metal  
537 pollution in the Amvrakikos Bay, *Gl. Nes.* 21, 7-13, <https://doi.org/10.30955/gnj.002733>, 2019.

538

539 Gredilla, A., Stoichev, T., Fdez-Ortiz de Vallejuelo, S., Rodriguez-Iruretagoiena, A., Morais, P., Arana, G., and Madariaga,  
540 J.M.: Spatial distribution of some trace and major elements in sediments of the Cávado estuary (Esposende, Portugal), *Mar.*  
541 *Poll. Bull.*, 99, 305–311, <https://doi.org/10.1016/j.marpolbul.2015.07.040>, 2015.

542





- 543 Hahladakis, J., Smaragnaki, E., Vasilaki, G., and Gidaragos, E.: Use of Sediment Quality Guidelines and pollution indicators  
544 for the assessment of heavy metal and PAH contamination in Greek surficial sea and lake sediments, *Env. Mon. Assess.*,  
545 185, 2843–2853, 10.1007/s10661-012-2754-2, 2012.
- 546
- 547 Jackson, M.L.: Soil Chemical Analysis, *S. Sc. Soc. of Am. J.*, 22, 272-272,  
548 <https://doi.org/10.2136/sssaj1958.03615995002200030025x>, 1958.
- 549
- 550 Karageorgis, A.P., Kaberi, H., Price, N.B., Muir, G.K.P., Pates, J.M., and Lykousis, V.: Chemical composition of short  
551 sediment cores from Thermaikos Gulf (Eastern Mediterranean): Sediment accumulation rates, trawling and winnowing  
552 effects, *Cont. Sh. Res.*, 25, 2456–2475, <https://doi.org/10.1016/j.csr.2005.08.006>, 2005.
- 553
- 554 Kelepertsis, A., Alexakis, D., and Kita, I.: Environmental Geochemistry of soils and waters of Susaki Area, Korinthos,  
555 Greece, *Env. Geoch. and H.*, 23, 117-135, 2001.
- 556
- 557 Kontoyiannis, H.: Observations on the circulation of the Saronikos Gulf: A Mediterranean embayment sea border of Athens,  
558 *Geoph. Res.*, 115, 10.1029/2008JC005026, 2010.
- 559
- 560 Long, E.R., MacDonald, D.D., Smith, S.L., and Calder, F.D.: Incidence of Adverse Biological Effects Within Ranges of  
561 Chemical Concentrations in Marine and Estuarine Sediments, *Env. Manag.*, 19, 81-97, <https://doi.org/10.1007/BF02472006>,  
562 1995.
- 563
- 564 Loring, H.D., and Rantala, R. : Manual for the Geochemical Analyses of Marine Sediments and Suspended Particulate  
565 Matter. *E. Sc.*, 32, 235-283, [http://dx.doi.org/10.1016/0012-8252\(92\)90001-A](http://dx.doi.org/10.1016/0012-8252(92)90001-A), 1992.
- 566
- 567 Manahan, E.: *Water Chemistry, Green Science and Technology of Nature's Most Renewable Resource*, 1<sup>st</sup> edition, CRC  
568 Press, Taylor & Francis Group, U.S., 416 pp., 2011.
- 569
- 570 Nolting, R.F., Ramkema, A., and Everaarts, J.M.: The geochemistry of Cu, Cd, Zn, Ni and Pb in sediment cores from the  
571 continental slope of the Banc d'Arguin (Mauritania), *Cont. Sh. Res.*, 19, 665 -691,  
572 [ui.adsabs.harvard.edu/link\\_gateway/1999CSR....19..665N/doi:10.1016/S0278-4343\(98\)00109-5](http://ui.adsabs.harvard.edu/link_gateway/1999CSR....19..665N/doi:10.1016/S0278-4343(98)00109-5), 1999.
- 573
- 574 Ozturk, M.: Trends of trace metal (Mn, Fe, Co, Ni, Cu, Zn, Cd and Pb) distributions at the oxic-anoxic interface and in  
575 sulfidic water of the Drammensfjord, *Mar. Chem.*, 48, 329-342, [https://doi.org/10.1016/0304-4203\(95\)92785-Q](https://doi.org/10.1016/0304-4203(95)92785-Q), 1995.
- 576
- 577 Panagopoulou, G., Heavy metals (Hg, Pb, Cd) at water samples and sediments of Saronikos Gulf, MSc thesis, University of  
578 Athens in Greece, Greece, 2018.
- 579
- 580 Paraskevopoulou, V.: Distribution and chemical behaviour of heavy metals in sea area affected by industrial pollution (NW  
581 Saronikos), PhD Thesis in Chemical Oceanography, University of Athens in Greece, Greece, 2009.
- 582
- 583 Paraskevopoulou, V., Zeri, C., Kaberi, H., Chalkiadaki, O., Krasakopoulou, E., Dassenakis, M., and Scoullou, M.: Trace  
584 metal variability, background levels and pollution status assessment in line with the water framework and Marine Strategy



585 Framework EU Directives in the waters of a heavily impacted Mediterranean Gulf, *Mar. Poll. Bull.*, 87, 323-337,  
586 10.1016/j.marpolbul.2014.07.054, 2014.  
587  
588 Peña-Icart, M., Villanueva, M., Alonso Hernández, C., Rodríguez Hernández, J, Behar, M., and Pomares Alfonso, M.:  
589 Accepted Manuscript, Comparative Study of Digestion Methods EPA 3050B (HNO<sub>3</sub>-H<sub>2</sub>O<sub>2</sub>-HCl) and ISO 11466.3 (aqua  
590 regia) for Cu, Ni and Pb Contamination Assessment in Marine Sediments, *Mar. Env. R.*, 60-66, [https://hal.archives-](https://hal.archives-ouvertes.fr/hal-00720186/document)  
591 [ouvertes.fr/hal-00720186/document](https://hal.archives-ouvertes.fr/hal-00720186/document), 2011.  
592  
593 Pohl, C., and Hennings, U.: The effect of redox processes on the partitioning of Cd, Pb, Cu, and Mn between dissolved and  
594 particulate phases in the Baltic Sea, *Mar. Chem.*, 65, 41-53, [https://doi.org/10.1016/S0304-4203\(99\)00009-2](https://doi.org/10.1016/S0304-4203(99)00009-2), 1999.  
595  
596 Skoog, D., Holler, F.J., and Nieman, T. A.: Principles of Instrumental Analysis, Fifth Edition, Saunders golden sunburst  
597 series, Saunders College Pub., Philadelphia , Orlando, Fla., Harcourt Brace College Publishers, 1998.  
598  
599 Sutherland, R.A.: Bed sediment-associated trace metals in an urban stream, Oahu, Hawaii, *Env. Geol.*, 39, 611-627, [https://](https://doi.org/10.1007/s00250050473)  
600 [doi.org/10.1007/s00250050473](https://doi.org/10.1007/s00250050473), 2000.  
601  
602 Tsoutsia, A., Kapsimalis, V., Poulos , S., Paraskevopoulou, V., and Dassenakis, E.: Assessment of heavy metals  
603 contamination in the coastal sediments of the broader area of Chios Harbor (Aegean Sea), Proceedings of the 13th  
604 International Congress, Exploration and exploitation of Mineral Sources, Chania, Greece, 5-8 September 2013, 1581-1589,  
605 10.12681/bgsg.11001, 2013.  
606  
607 Vrettou, E.: Heavy metals in sediment cores of Saronikos Gulf, MSc thesis, University of Athens in Greece, Greece, 2019.  
608  
609 Walkley, A.: A Critical Examination of a Rapid Method for Determining Organic Carbon in Soils: Effect of Variations in  
610 Digestion Conditions and of Inorganic Soil Constituents. *Soil Sc.*, 63, 251-264,  
611 <http://dx.doi.org/10.1097/00010694-194704000-00001>, 1947.  
612  
613 Xarlis, P.: Heavy metals (Cu, Ni, Zn) at water samples and sediments of Saronikos Gulf, MSc thesis, University of Athens in  
614 Greece, Greece, 2018.  
615  
616  
617  
618  
619  
620  
621  
622  
623  
624  
625  
626  
627